NACA

RESEARCH MEMORANDUM

INVESTIGATION AT MACH NUMBER 2.93 OF HALF OF A CONICAL-SPIKE DIFFUSER MOUNTED AS A SIDE INLET WITH BOUNDARY-LAYER CONTROL

By Thomas G. Piercy and Harry W. Johnson

Lewis Flight Propulsion Laboratory
Cleveland, Ohio

NATIONAL ADVISORY COMMITTEE
FOR AERONAUTICS

WASHINGTON
September 10, 1952

NATIONAL ADVISORY COMMITTEE FOR AERONAUTICS

RESEARCH MEMORANDUM

INVESTIGATION AT MACH NUMBER 2.93 OF HALF OF A CONICAL-SPIKE DIFFUSER MOUNTED AS A SIDE INLET WITH BOUNDARY-LAYER CONTROL

By Thomas G. Piercy and Harry W. Johnson

SUMMARY

An experimental investigation was conducted to determine the performance characteristics of a side inlet with boundary-layer control operating in the presence of laminar and turbulent initial boundary layers at a free-stream Mach number of 2.93. The inlet was alined at zero angle of attack and yaw with respect to the local free stream.

The inlet consisted of half of a 60° conical-spike supersonic diffuser, which was mounted on a flat plate and designed for all-external compression, and a subsonic diffuser which faired into a simulated cylindrical combustion chamber. Removal of the flat-plate boundary layer ahead of the inlet was accomplished by means of a variable-height, ram-type boundary-layer scoop having a straight leading edge positioned at the diffuser spike tip.

The greatest inlet total-pressure recovery obtained in the presence of the turbulent boundary layer was approximately 51.5 percent when the boundary-layer-scoop height was equal to approximately 0.88 boundary-layer thickness. Inlet peak pressure recovery was reduced to 36.7 percent when the entire turbulent boundary layer was allowed to enter the inlet.

The peak pressure recoveries observed in the presence of the initial laminar boundary layer varied from 39.7 percent with no boundary-layer removal to 45.8 percent at the largest value of the scoop height tested (1.446 boundary-layer thicknesses). At the larger values of scoop height tested, the inlet pressure recovery approached that obtained with the initial turbulent boundary layer, as expected. For scoop heights equal to or less than the boundary-layer thickness, the pressure recovery was generally lower than that obtained with the turbulent boundary layer because of the inherent inability of the scoop to capture a full projected stream tube of air when operated in the presence of the laminar boundary layer. In addition, the apparently favorable effect of allowing small amounts of turbulent boundary layer to enter the inlet could not be realized.

Inlet total-pressure recovery decreased markedly with reduced boundary-layer-scoop mass flow. Inlet stability was sensitive to subcritical scoop operation, particularly at the larger scoop heights investigated for the turbulent boundary layer and for all scoop heights investigated for the laminar boundary layer.

INTRODUCTION

The side inlet must operate in the presence of the flow field and boundary layer over the surface on which it is installed. Research conducted in the Mach number range from about 1.5 to 2.0 has indicated that side-inlet performance can be made comparable to nose-inlet performance by suitable control of the initial boundary layer. Boundary-layer removal has been employed successfully in this respect (references 1 to 4).

This investigation was conducted at the NACA Lewis laboratory to extend the study of side-inlet performance with various amounts of boundary-layer removal to a free-stream Mach number of about 3.0. The side inlet consisted of half of a single-shock conical-spike supersonic inlet mounted on a flat plate and alined at zero angle of attack and yaw with respect to the local free stream. Boundary-layer removal was accomplished with a variable-height ram-type scoop with a straight leading edge positioned at the spike tip.

The initial boundary layer at the inlet was varied by changing the plate length upstream of the inlet. Transition to turbulent flow was forced on the longest plate by roughness added near the plate leading edge. Both the inlet and the boundary-layer scoop were operated over a range of mass-flow ratios at various scoop heights in both laminar and turbulent boundary layers.

SYMBOLS

The following symbols are used in this report:

A	area
h	height of boundary-layer-removal scoop above flat plate
h/δ	dimensionless boundary-layer-scoop-height parameter
L	plate length, measured from leading edge to spike tip
L/R	dimensionless plate-length parameter
m	mass flow

P	total pressure
R	inlet radius, measured from center line of spike to cowl lip, 1.5 in.
V	velocity
x	lineal distance, parallel to plate, measured from cowl-lip station
y	normal distance above plate
δ	boundary-layer thickness, distance from surface to point in boundary layer where velocity is equal to 0.99 free-stream velocity
δ/R	dimensionless boundary-layer-thickness parameter
δ^*/θ	boundary-layer-form factor, the quotient of boundary-layer displacement and momentum thicknesses

Subscripts:

D	inlet
max	maximum
S	boundary-layer scoop
T	throat
0	free-stream conditions
1	conditions 1/2 inch upstream of spike tip
2	conditions at exit of diffuser or boundary-layer scoop

APPARATUS AND PROCEDURE

The side inlet illustrated in figure 1 was tested in the 18- by 18-inch Mach number 3.05 tunnel at the NACA Lewis laboratory. The model was alined at zero angle of attack (except for slight flow angularity caused by boundary-layer growth) and zero yaw with respect to the local free stream which, because of an inclination of the plate, had a Mach number of 2.93. The inlet model was the same one described in reference 3, except for subsequently described changes in the cowl lip and spike centerbody.

Engine induction system. - The inlet consisted of half of an axially symmetric 60° conical-spike supersonic diffuser designed for all-external compression (no internal contraction) mounted on a flat plate. The spike and cowl lip were designed for maximum pressure recovery and zero spillage at a Mach number of 3.15; but at a Mach number of 2.93 the conical shock wave originating at the cone apex passed upstream of the cowl lip, permitting approximately 7-percent spillage with the inlet operating supercritically. The cowl-lip angle was small enough to ensure shock attachment during supercritical operation at a Mach number of 2.93. Important design details and dimensions of the side-inlet configuration are presented in figure 2(a).

The subsonic diffuser was faired into a simulated cylindrical combustion chamber, the axis of which was displaced 0.4 inlet radius inboard of the spike axis in an attempt to simulate a practical side-inlet installation. Subsonic-diffuser area variations are presented in figure 2(b). The pressure instrumentation (fig. 3) consisted of 41 total-pressure tubes (all tubes except the center tube were located at the centroids of equal areas), 4 static-pressure tubes, and 4 wall static-pressure orifices. This instrumentation was located at station 2, which was approximately 2.1 combustion-chamber diameters downstream of the combustion-chamber entrance. Pressures recorded at this station were used to determine combustion-chamber total pressure and Mach number. The inlet mass flow was varied by a movable plug at the combustion-chamber exit (see fig. 4) and was discharged into the tunnel subsonic diffuser.

Boundary-layer-removal system. - The boundary-layer-removal system consisted of a simple ram-type scoop with straight leading edge positioned at the spike tip, as described in reference 3. Boundary-layer mass flow was controlled and measured by a system of rotameters as shown in figure 4 and was discharged into the top of the tunnel test section. A surge tank was inserted in the ducting ahead of the rotameters to help stabilize the rotameter readings during unstable operating conditions. Total pressures in the boundary-layer duct were measured with a 17-tube rake.

Test conditions. - The free-stream Mach number 1/2-inch upstream of the spike tip (at station 1) was determined from pressure measurements to be 2.93, and was considered to be the local free-stream Mach number at the inlet. Test-section total temperature and pressure were approximately 200° F and atmospheric, respectively, which produced a Reynolds number of approximately 1.55×10^6 per foot. The dew point was maintained within the range of -20° to -10° F, which ensured negligible water-condensation effects.

Boundary-layer variation and measurement. - Variation of the initial boundary layer was accomplished by changing the length of the flat plate upstream of the inlet. Plate-length parameters L/R of approximately 7.67 and 9.67 were used to obtain laminar and turbulent boundary layers,

respectively. Transition to turbulent boundary layer was forced on the longer plate by a 1-inch strip of number 100 carborundum dust sprinkled lightly on wet lacquer. This strip was located 1/2 inch from the plate leading edge.

The boundary layers were surveyed with the instrumentation shown in figures 2(a) and 5. Four movable pitot tubes and three static orifices in the plate located at station 1 were used to obtain total-pressure and Mach-number profiles ahead of the inlet. All boundary-layer data were reduced under the assumption of a zero normal static-pressure gradient within the boundary layer.

The nondimensional boundary-layer velocity profiles presented in figure 5 represent average conditions in the transverse plane at station 1. The velocity ratio V/V_0 is plotted as a function of the parameter y/δ, where δ is the height within the boundary layer at which the velocity is 0.99 free-stream velocity. Boundary-layer form factors δ^*/θ computed for these profiles were 7.55 and 5.05 for the laminar and turbulent layers, respectively. Boundary-layer-thickness parameters δ/R, in terms of inlet lip radius R, were 0.075 and 0.160, respectively.

Test variables. - Boundary-layer-scoop height was varied from zero to a value greater than the boundary-layer thickness for each initial boundary layer. Inlet mass flow was varied from supercritical to subcritical operation, and boundary-layer-scoop mass flow was varied from zero to the maximum attainable for each combustion-chamber Mach number (constant exit area) investigated.

In the following discussions the terms "supercritical" and "subcritical" are applied to inlet and boundary-layer-scoop operation, and are defined as follows: With supercritical operation the inlet or scoop captures its maximum mass flow and operates with a swallowed normal shock; with subcritical operation the captured mass flow is reduced. Supercritical operation does not necessarily imply that the inlet or scoop is capturing a full projected stream tube of air, however, since pressure feedback through the boundary layer or interaction effects may reduce the maximum attainable mass flow.

The assumption of sonic-flow velocity at the minimum geometric exit area made possible the calculation of inlet mass flow m_D from the total-pressure measurements at station 2. The variation of inlet total-pressure recovery $P_{2,D}/P_{1,D}$ as a function of inlet mass-flow ratio $m_D/m_{1,D}$ was obtained for each scoop operating condition. For supercritical scoop operation it was possible to estimate that portion of the curve corresponding to supercritical inlet operation. This portion of the curve was corrected to correspond with the known mass flow in the captured

stream tube at station 1. A discharge coefficient was thus obtained as a function of combustion-chamber Mach number for each boundary-layer-scoop-height parameter h/δ. These coefficients were then used to correct the supercritical portions of the inlet performance curves obtained at reduced scoop mass flow. The discharge coefficient for critical inlet operation was assumed to apply throughout the subcritical inlet operating region.

Some possibility of error existed in the determination of scoop mass flow because of the use of rotameters at pressures slightly below their calibrated range. The scoop mass flow was not corrected, however, since there was a possibility that pressure feedback caused thickening of the boundary layer ahead of the scoop, decreasing the maximum attainable scoop mass flow.

Pressures were recorded photographically on tetrabromoethane multimanometer boards. Schlieren photographs and high-speed motion pictures were taken of the flow in the vicinity of the inlet.

DISCUSSION OF RESULTS

Mass-Flow and Total-Pressure Referencing

Inlet total-pressure recovery and mass-flow ratio were referenced to conditions at station 1, which is a nonuniform flow field due to the presence of the boundary layer. The total pressure $P_{1,D}$ represents the average total pressure at station 1 in the stream tube captured by the inlet with supercritical operation. For all boundary-layer-scoop-height parameters h/δ less than about 1.4, a portion of the low-energy boundary layer enters the inlet, and thus $P_{1,D}$ is a function of h/δ. The variation of $P_{1,D}/P_0$ with h/δ, where P_0 is the free-stream total pressure, was obtained from the total-pressure profile at station 1 by means of an area-weighting technique and is presented in figure 6(a). Similarly, the inlet reference mass flow $m_{1,D}$, which represents the mass flow at station 1 in the stream tube captured by the inlet when supercritical conditions are assumed, was also determined by an area-weighting method. (Because of spillage, $m_{1,D}$ in this case is approximately 7 percent less than that corresponding to the capture of a full projected stream tube.) The ratio $m_{1,D}/m_{0,D}$, where $m_{0,D}$ represents the corresponding inlet mass flow in the free stream, is also shown in figure 6(a) as a function of h/δ.

Similar data for the boundary-layer scoop are presented in figure 6(c). In addition, the mass-flow ratio $m_{1,(D+S)}/m_{0,(D+S)}$ and total-pressure ratio $P_{1,(D+S)}/P_0$ for the combined inlet and boundary-layer scoop are

shown in figure 6(b) as functions of h/δ. These various relations make it possible to reference data to free-stream conditions if desired.

These ratios were obtained when supercritical operation of the inlet and scoop was assumed. During conditions of buzz these ratios would obviously vary. However, since no method was available for determining variations during buzzing conditions, these ratios were arbitrarily used to reference both steady and buzzing conditions.

With no removal of the turbulent boundary layer ($h/\delta = 0$), the available inlet mass-flow ratio $m_{1,D}/m_{0,D}$ and total-pressure ratio $P_{1,D}/P_0$ were 93 and 88 percent, respectively, as indicated in figure 6(a). These values are lower than those presented for a comparable turbulent boundary-layer-thickness parameter in reference 3 because of the higher free-stream Mach number of the present investigation. At h/δ of zero for the laminar boundary layer, the available inlet mass-flow ratio $m_{1,D}/m_{0,D}$ and total-pressure ratio $P_{1,D}/P_0$ were 95 and 93 percent, respectively. That these values are larger than the corresponding values for the turbulent layer may be attributed to the smaller laminar boundary-layer thickness.

Visual-Flow Observations

Peak pressure recovery. - Schlieren photographs of the inlet operating near peak pressure recovery were taken at 1/100-second exposure, and are presented in figure 7 for each value of h/δ tested. The flow represented is steady for the turbulent boundary layer at all values of h/δ except 0 and 1.510, whereas the flow is unsteady for the laminar boundary layer at all values of h/δ except 0, 1.284, and 1.446. The weak oblique wave originating on the plate just upstream of the inlet was produced by a junction in the plate and had no effect on the flow at the inlet. The oblique waves originating at the plate leading edge were caused by the small angle of attack at which the plate was set relative to the tunnel free stream, and, on the longer plate, by the carborundum dust strip used to force transition.

Unsteady flow, inlet operation in presence of turbulent boundary layer. - The shock oscillations observed for the inlet operating in the presence of the turbulent boundary layer depended on combinations of inlet and scoop operating conditions and on the boundary-layer-scoop-height parameter h/δ. In general, however, the patterns observed for given inlet-scoop operating conditions did not vary for h/δ greater than 0.833. For these higher h/δ values, distinct types of oscillation occurred for the following operating conditions:

(a) Subcritical inlet, supercritical scoop operation. The buzz pattern indicated in figure 8(a) is similar to that observed during subcritical operation of spike-type-nose inlets. The normal shock oscillated onto the spike a distance depending on the degree of subcritical inlet operation.

(b) Subcritical operation of both scoop and inlet. As indicated in figure 8(b), the shock oscillation extended to the plate leading edge for large degrees of subcritical operation, with separation of the boundary layer occurring behind the shock.

(c) Supercritical inlet, subcritical scoop operation. For this condition, as illustrated in figure 8(c), scoop buzz was rapid but did not extend far upstream of the inlet. No flow separation or inlet cowl-lip-shock detachment was observed.

(d) Inlet operating supercritically near peak pressure recovery, subcritical scoop operation. In this case inlet buzz was induced by scoop buzz, although the oscillating cowl-lip shock did not extend beyond the spike tip. Some flow separation was observed, as illustrated in figure 8(d).

The buzz patterns observed at lower values of h/δ in the turbulent boundary layer did not correspond exactly to those just described for comparable operating conditions. Exceptions were as follows:

(a) Subcritical inlet operation with no boundary-layer removal, h/δ of 0. This condition was characterized by shock oscillations onto the plate with flow separation occurring behind the shock. The cowl-lip shock persisted, as indicated in figure 8(e), except for extreme subcritical operation.

(b) Subcritical operation of inlet and scoop at h/δ of 0.509 and 0.667. In contrast to the same operating condition at higher h/δ (fig. 8(b)), flow separation was not observed but may have existed to some extent at these values of h/δ. A rapid oscillation of the cowl-lip shock occurred, and at greatly reduced inlet mass flows this shock disappeared while the oblique shock moved farther out onto the plate. This condition is illustrated in figure 8(f).

(c) Subcritical inlet operation with supercritical scoop operation at h/δ of 0.509 and 0.667. This operation was characterized by shock oscillations quite similar to the pattern already identified in figure 8(f). In contrast with comparable operating conditions at higher h/δ, the cowl-lip shock oscillated but did not disappear until the inlet was operated at greatly reduced mass flows. Flow separation was not observed.

(d) Supercritical inlet operation with subcritical scoop operation, h/δ of 0.509. For this condition no detachment of the lip shock was noted, and the oblique shock moved farther out on the plate than was observed for comparable conditions at the higher values of h/δ as given in figure 8(c).

(e) Supercritical inlet operation with subcritical scoop operation, h/δ of 0.667. Subcritical scoop operation was associated with considerable travel of the oblique shock and oscillation of the cowl-lip shock, indicating inlet buzz induced by scoop buzz. However, no separation of the boundary layer behind the oblique shock was observed.

As a point of interest, it was noted when separation of the boundary layer was observed that static-pressure rises across the oblique shocks obtained from measured shock angles were only slightly greater than the critical value predicted in reference 5 for turbulent boundary layers at Reynolds numbers based on plate length. Similarly, the static-pressure rises across the oblique shocks when separation was not observed were calculated to be slightly less than the predicted critical value.

Unsteady flow, inlet operation in presence of laminar boundary layer. - Buzz patterns observed in the presence of the laminar boundary layer were similar to those just described, with one notable exception; that is, when buzzing occurred it was always accompanied by separation of the boundary layer behind the oblique shocks. With the inlet operating supercritically, no scoop buzz was noticed with subcritical scoop operation unless the scoop mass flow was reduced to almost zero. Indications of usual spike-type-nose-inlet buzz were observed for values of h/δ greater than 0.705. Therefore, the buzz patterns for the laminar boundary layer may be represented by figures 8(a) to 8(c).

Inlet Performance

Pressure and Mach-number variations across station 2 were small for every operating condition investigated. At peak pressure recovery and at high-pressure-recovery supercritical inlet operation, the maximum variation in total pressure among the individual tubes of the rake was less than 1 percent. With boundary-layer-scoop mass-flow ratio reduced to 50 percent, this variation did not exceed 1.5 percent. No boundary-layer separation at the rake station was observed, in contrast to the findings of reference 3. This absence of boundary-layer separation is thought to be due primarily to the large amount of subsonic diffusion provided by this diffuser. However, this observation does not preclude the possibility of separation between the inlet lip and the rake station, inasmuch as boundary-layer reattachment may occur at the low subsonic Mach numbers. Combustion-chamber-inlet Mach numbers of the order of 0.10 were observed at peak pressure recovery.

Boundary-layer-scoop mass flow was varied from the maximum attainable to zero for several values of the combustion-chamber Mach number at each value of h/δ investigated. These data yielded inlet total-pressure recovery $P_{2,D}/P_{1,D}$ as a function of scoop mass-flow ratio $m_S/m_{S,max}$. These values are presented in figure 9 as a function of inlet mass-flow ratio $m_D/m_{1,D}$ for the turbulent boundary layer. For all values of h/δ except 1.510, the scoop mass-flow ratio presented is $m_S/m_{S,max}$, where $m_{S,max}$ represents the maximum supercritical scoop mass flow captured at that particular value of combustion-chamber Mach number.

Lines of constant combustion-chamber Mach number are indicated in figure 9(b) for h/δ of 0.509. It should be noted that the scoop mass-flow ratio designated at any point (i.e., given combustion-chamber Mach number) represents a percentage of the maximum captured at that particular value of combustion-chamber Mach number. The variation of the maximum captured scoop mass flow as a function of combustion-chamber Mach number is indicated by the insert on figure 9(b). It is obvious from this insert that the maximum captured scoop mass flow decreased considerably when the inlet was operated subcritically. At h/δ of 1.510, the scoop would not operate supercritically, and the scoop mass-flow ratio was referenced to the calculated supercritical value $m_{1,S}$.

For large values of boundary-layer-scoop mass-flow ratio, the inlet performance curves (pressure recovery as a function of mass-flow ratio) were similar in form to those usually obtained for spike-type nose inlets. Peak pressure recoveries occurred at inlet mass-flow ratios slightly less than unity, although no clearly defined bow shock was observed; and at every value of h/δ greater than zero, inlet buzz occurred for inlet mass-flow ratios slightly less than those corresponding to peak pressure recoveries. At h/δ of zero, however, peak pressure recovery was obtained during slight inlet buzz. Further reductions in inlet mass flow increased the severity of buzz and were accompanied by reduced pressure recoveries. Regions of unsteady inlet operation are indicated in figure 9 by the dashed curves. During subcritical inlet operation the shock oscillations were frequently quite large; therefore some question exists as to the significance of manometer board readings for these operating conditions.

For all values of h/δ, reduction of boundary-layer-scoop mass flow decreased the inlet peak pressure recovery and supercritical mass flow and, in general, reduced the inlet mass-flow ratio at which peak pressure recovery occurred.

At h/δ of 0.509, reductions in boundary-layer-scoop mass flow did not affect inlet stability to any great extent. Peak pressure recovery at all values of scoop mass flow was obtained with the same value of combustion-chamber Mach number (except for zero scoop mass flow), and

no inlet buzz was noted. At values of h/δ of 0.667 and larger, however, a small amount of boundary-layer-scoop mass-flow reduction immediately threw the inlet into an unsteady condition. (This change in inlet stability between values of h/δ of 0.509 and 0.607 was introduced previously in the section describing the visual-flow observations.) This effect persisted at the larger values of h/δ, but was apparently most pronounced between h/δ values of 0.6 and 1.0.

The boundary-layer scoop could not be operated supercritically at h/δ of 1.510 in the turbulent boundary layer. Inlet pressure recoveries were therefore lower than anticipated. While this effect is not completely understood, it is believed that it could be caused by the metering system employed in the scoop ducting, and is thought not to be characteristic of an actual installation. The maximum scoop mass-flow ratios $m_s/m_{1,s}$ obtained at this h/δ are indicated on figure 9(f).

A summary plot of inlet peak pressure recovery as a function of scoop-height parameter h/δ and scoop mass-flow ratio is presented in figure 10 for the turbulent boundary layer. Peak pressure recovery of 51.5 percent at h/δ of approximately 0.88 was found by fairing between the observed values obtained at h/δ of 0.833 and 1.025. The value of h/δ at peak pressure recovery is believed consistent with the values indicated for maximum recovery at reduced scoop mass flow. Since the inlet pressure recovery predicted by shock theory was approximately 61 percent, it is indicated that additional shock or viscous effects or both accounted for a 9.5-percent loss in pressure recovery in the subsonic diffuser. Actually it was not established that the normal-shock configuration stabilized at the design throat Mach number. This condition is possible even though a slightly reduced mass flow was indicated at peak pressure recovery. In unpublished two-dimensional flow studies made at the Lewis laboratory, some reduction in mass flow at peak pressure recovery has been observed with the major portion of an extended shock pattern occurring downstream of the throat.

Peak pressure recovery decreased as h/δ was increased from 0.88. The fact that peak pressure recovery occurred with a portion of the turbulent boundary layer entering the inlet is not completely understood but is thought to result from a favorable effect of allowing a small amount of turbulent boundary layer to enter the diffuser throat. Similar effects were noted in reference 3.

Peak pressure recovery also decreased as h/δ was decreased from 0.88, such that at h/δ of 0, peak pressure recovery was only about 37 percent. Since a reduction in h/δ allows more of the flat-plate boundary layer to enter the inlet, the adverse effects of entering boundary layer on the inlet performance is obvious.

At values of h/δ less than approximately 0.55 in the turbulent boundary layer, the inlet peak pressure recovery decreased almost linearly with decreasing scoop mass-flow ratio. (This characteristic is associated with the fact that at the lower values of h/δ inlet stability was not affected by subcritical scoop operation.) This linear decrease, also reported in reference 3, is thought to be a function of the height of the boundary-layer-scoop lip stagnation streamline. At any value of h/δ, this height decreases as scoop mass flow decreases, and an increasing amount of boundary-layer air is spilled into the inlet. Operation at reduced scoop mass-flow ratio at any value of h/δ within this range is therefore comparable to operation with supercritical scoop at a lower value of h/δ.

At values of h/δ greater than approximately 0.55 in the turbulent boundary layer, subcritical scoop operation induced inlet instability, as mentioned previously. The effects of this instability are clearly indicated in figure 10. Pressure recovery for a given subcritical scoop mass flow decreases sharply when h/δ is increased slightly above 0.55, but as h/δ is further increased the pressure recovery increases again. The effects of subcritical scoop operation on the inlet stability are apparently most pronounced between h/δ values of 0.6 and 1.0, but were observed for scoop mass-flow ratios less than 96 percent for values of h/δ greater than 0.66. In comparison with similar results reported in reference 3, it was noted in the present investigation that this instability region occurred at lower values of h/δ and that larger values of the scoop mass-flow ratio were required to ensure stability.

Inlet peak pressure recoveries were obtained with supercritical scoop operation at every h/δ investigated, in constrast to the results of reference 3, in which it was observed that peak pressure recovery was obtained at slightly reduced scoop mass-flow ratios at large values of h/δ.

A comparison of inlet peak pressure recovery as a function of boundary-layer-scoop-height parameter for the laminar and turbulent boundary layers is presented in figure 11. Pressure recovery at h/δ of 0.705 in the laminar boundary layer was lower than that obtained at h/δ of 0.362 because the boundary-layer scoop captured less mass flow at the larger h/δ. Increases in pressure recovery at values of h/δ between 0.705 and 1.048 were due to the increased scoop mass flow captured. The boundary-layer scoop could not be made to operate supercritically for any value of h/δ less than 1.284; therefore the inlet pressure recoveries are generally lower for the laminar boundary layer than for the turbulent boundary layer at corresponding values of h/δ. The scoop operated supercritically at the two largest values of h/δ investigated for the laminar boundary layer. The highest inlet peak pressure recovery obtained for this boundary layer was 45.8 percent at h/δ of 1.446, the largest h/δ investigated.

With the assumption that supercritical scoop operation could be achieved with the initial turbulent boundary layer at large values of h/δ in an actual installation, it is evident from figure 11 that the inlet performance with initial laminar boundary layer approaches that of the initial turbulent boundary layer with increasing values of h/δ, as would be expected.

Peak pressure recovery was 39.7 percent when all the laminar boundary layer flowed into the inlet ($h/\delta = 0$). This recovery was slightly greater than that for the corresponding case for the turbulent boundary layer (36.7 percent) primarily because the laminar boundary layer was much thinner.

The point of peak pressure recovery is not necessarily the most desirable point at which to operate a supersonic diffuser, particularly if this operation represents an unsteady condition. Steady operation regions with the turbulent boundary layer may be determined from figure 9. For the laminar boundary layer, the inlet total-pressure recovery as a function of inlet mass flow is presented in figure 12 for the maximum attainable scoop mass flow. Unstable inlet operation is represented by dashed lines. Stable inlet operation was achieved at peak pressure recovery only for the values of h/δ that permitted supercritical scoop operation and for h/δ of zero. For those values of h/δ where supercritical scoop flow could not be achieved, steady inlet operation was attained only with supercritical inlet mass flow.

Boundary-Layer-Scoop Performance

The boundary-layer scoop employed in this investigation was not entirely satisfactory, for it could not be operated supercritically for a number of operating conditions. Furthermore, large pressure-recovery losses were observed in the scoop system. Part of the reduced scoop performance is attributed to the area discontinuity within the duct $1\frac{1}{2}$ inches downstream of the scoop lip, a feature required in the scoop-height-adjustment method employed.

Scoop performance curves are presented in figures 13 and 14 for operation in the turbulent and laminar boundary layers, respectively. The data presented represent average performance with supercritical inlet operation. Scoop total-pressure recovery is plotted as a function of the scoop mass-flow ratio $m_S/m_{1,S}$. Figures 13(a) and 14(a) reference the scoop pressure recovery to conditions in the boundary layer at station 1, while figures 13(b) and 14(b) reference the pressure recovery to the local free-stream total pressure.

[redacted]

Scoop performance with turbulent boundary layer. - The performance curves for the turbulent boundary-layer operation (fig. 13) are similar to those presented in reference 3 and indicate that the scoop operated supercritically at all values of h/δ investigated except 1.510, as mentioned previously. Scoop buzz was observed for all values of h/δ at mass flows less than those corresponding to scoop peak pressure recovery.

The supercritical scoop mass flows measured indicate some disagreement with the theoretical supercritical values, the disagreement increasing with lower values of h/δ. While the accuracy of the measurements of mass flow through the rotameters was not determined, the trends observed are thought to be indicative of spillage caused by pressure feedback through the boundary layer. The ratio $m_{S,max}/m_{1,S}$ may be easily obtained from figure 13 for each h/δ, and the scoop mass-flow ratios presented in figure 9 may be converted to $m_S/m_{1,S}$ if desired.

Scoop performance with laminar boundary layer. - The scoop performance for operation in the laminar boundary layer indicates that only at the extremely large scoop-height settings could the scoop be made to operate supercritically. The small mass-flow ratios obtained, particularly at h/δ of 0.705, indicate considerable spillage. This subcritical operation is thought to be due largely to the inherent instability of the laminar boundary layer in the presence of adverse pressure gradients. In figure 2(a) it may be observed that the scoop design requires the flow to be turned immediately on entering the scoop. The shock originating at the scoop lip due to the upper surface 5.5° wedge angle provides an additional adverse pressure gradient which may cause an oscillating flow separation from the lower wall. It is possible that supercritical boundary-layer-scoop flow could have been obtained had it been possible to effect greater reductions in scoop back pressure.

For values of h/δ between 0.705 and 1.048, the amount of scoop spillage was reduced, and corresponding increases in inlet pressure recovery were produced, as mentioned previously. At h/δ values of 1.284 and 1.446, the scoop operated supercritically, causing further inlet pressure-recovery increases. At the larger values of h/δ in the laminar boundary layer, the energy level of the boundary layer entering the scoop is increased and approaches that of the turbulent boundary layer. Thus it is reasonable to expect that turbulent scoop performance would be approached and that supercritical scoop operation would occur.

To provide the designer with an insight as to how much boundary-layer air is available for cooling purposes, figure 15 is presented. Theoretical supercritical scoop-to-inlet mass-flow ratio is presented as a function of h/δ for both initial boundary layers.

[redacted]

SUMMARY OF RESULTS

An experimental investigation of the performance of a spike-type side inlet at a Mach number of 2.93 yielded the following results:

1. The maximum inlet total-pressure recovery observed was approximately 51.5 percent with the boundary-layer scoop operating supercritically in the initial turbulent boundary layer at a scoop height of 0.88 boundary-layer thickness. The highest pressure recovery observed with the inlet operating in the initial laminar boundary layer was approximately 45.8 percent with the boundary-layer scoop operating supercritically at the largest scoop height investigated (1.446 boundary-layer thicknesses).

2. Allowing all the initial boundary layer to flow into the inlet reduced the pressure recovery to 36.7 percent for the turbulent layer and to 39.7 percent for the laminar layer. The higher pressure recovery in the latter case was attributed to the smaller thickness and smaller total-pressure decrement of the laminar boundary layer. Most of the additional losses in pressure recovery were assumed to occur in the subsonic diffuser either as shock or viscous losses.

3. At the larger values of scoop height tested, the inlet pressure recovery with an initial laminar boundary layer approached that obtained with the turbulent boundary layer, although that of the former was generally lower because of the inherent inability of the scoop to capture a full projected stream tube of air when operated in the presence of the laminar boundary layer. In addition, the apparently favorable effect of allowing small amounts of turbulent boundary layer to enter the inlet could not be realized with the laminar boundary layer.

4. The inlet was quite sensitive to boundary-layer-scoop operation. Subcritical scoop operation reduced inlet pressure recovery and mass flow at every scoop height in both boundary layers, and induced inlet instability over a wide range of scoop heights in the turbulent boundary layer and over the entire range of scoop heights tested in the laminar boundary layer.

Lewis Flight Propulsion Laboratory
National Advisory Committee for Aeronautics
Cleveland, Ohio

REFERENCES

1. Edwards, Sherman S.: Experimental Investigation at Supersonic Speeds of Side Scoops Employing Boundary-Layer Suction. NACA RM A9I29, 1949.

2. Wittliff, Charles E., and Byrne, Robert W.: Preliminary Investigation of a Supersonic Scoop Inlet Derived from a Conical-Spike Nose Inlet. NACA RM L51G11, 1951.

3. Goelzer, H. Fred, and Cortright, Edgar M., Jr.: Investigation at Mach Number 1.88 of Half of a Conical-Spike Diffuser Mounted as a Side Inlet with Boundary-Layer Control. NACA RM E51G06, 1951.

4. Valerino, Alfred S.: Performance Characteristics at Mach Numbers to 2.0 of Various Types of Side Inlets Mounted on Fuselage of Proposed Supersonic Airplane. I - Two-Dimensional Compression-Ramp Inlets with Semicircular Cowls. NACA RM E52E02, 1952.

5. Donaldson, Coleman du P., and Lange, Roy H.: Study of the Pressure Rise Across Shock Waves Required to Separate Laminar and Turbulent Boundary Layers. NACA RM L52C21, 1952.

[redacted]

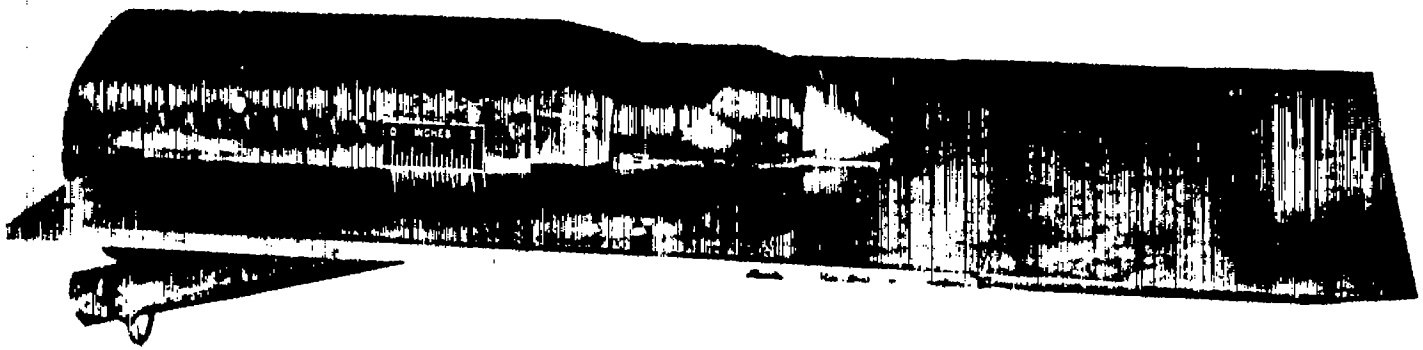

NACA
C-29062

Figure 1. - Conical-spike diffuser mounted as side inlet. Model removed from tunnel.

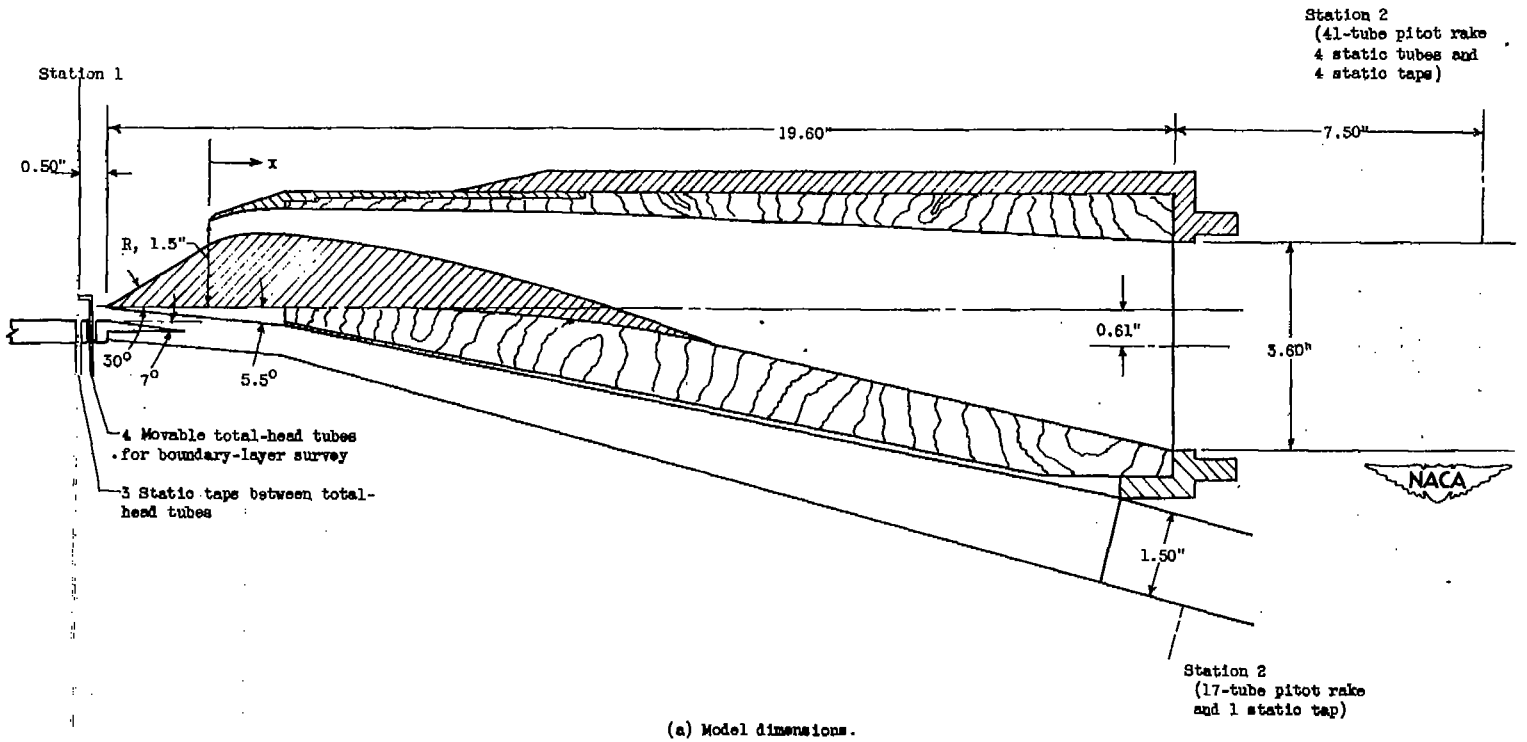

(a) Model dimensions.

Figure 2. - Dimensions and cross-section area variations of side-inlet configuration.

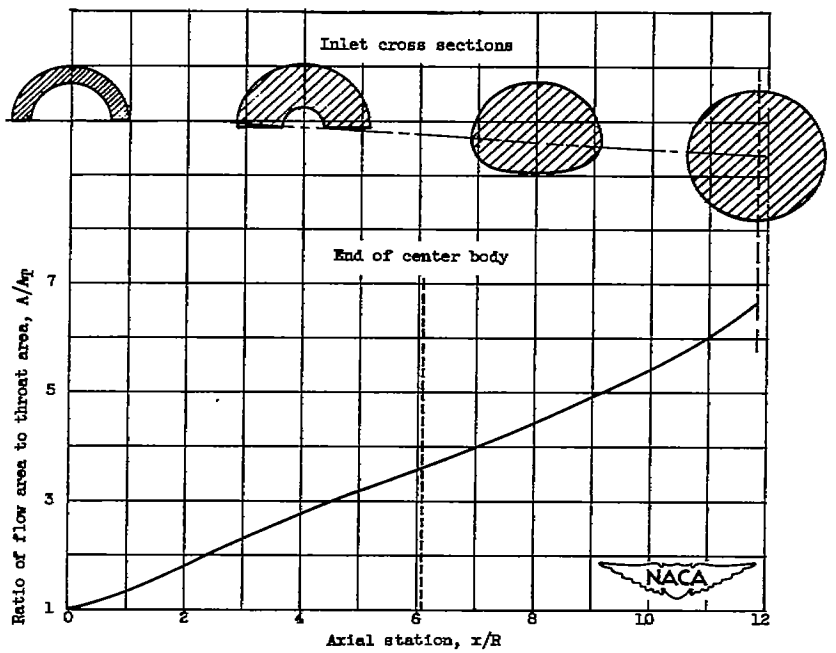

(b) Inlet-area distribution.

Figure 2. - Concluded. Dimensions and cross-section area variations of side-inlet configuration.

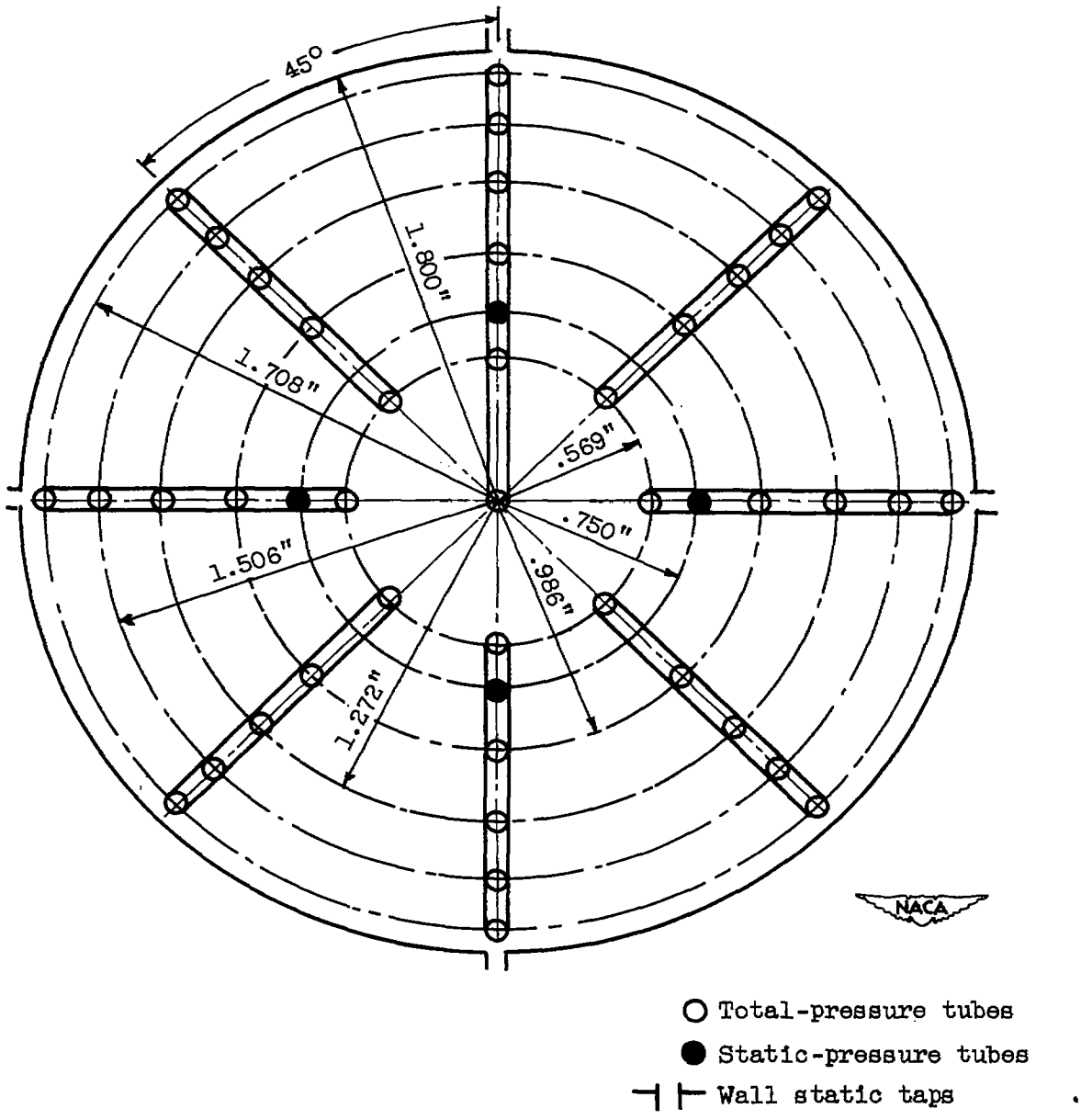

Figure 3. - Pressure-measurement instrumentation in diffuser.

[redacted]

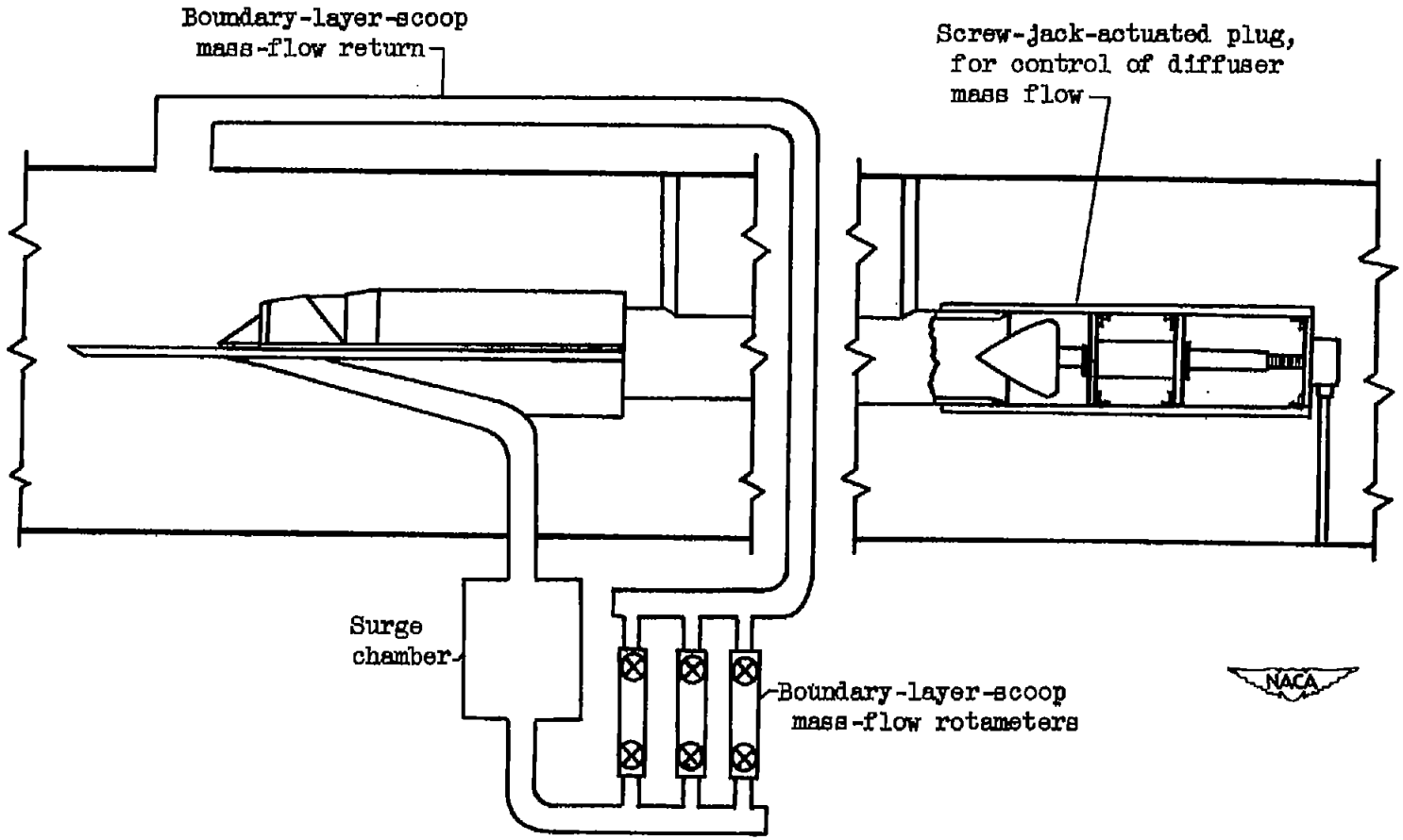

Figure 4. - Flow-measuring instrumentation.

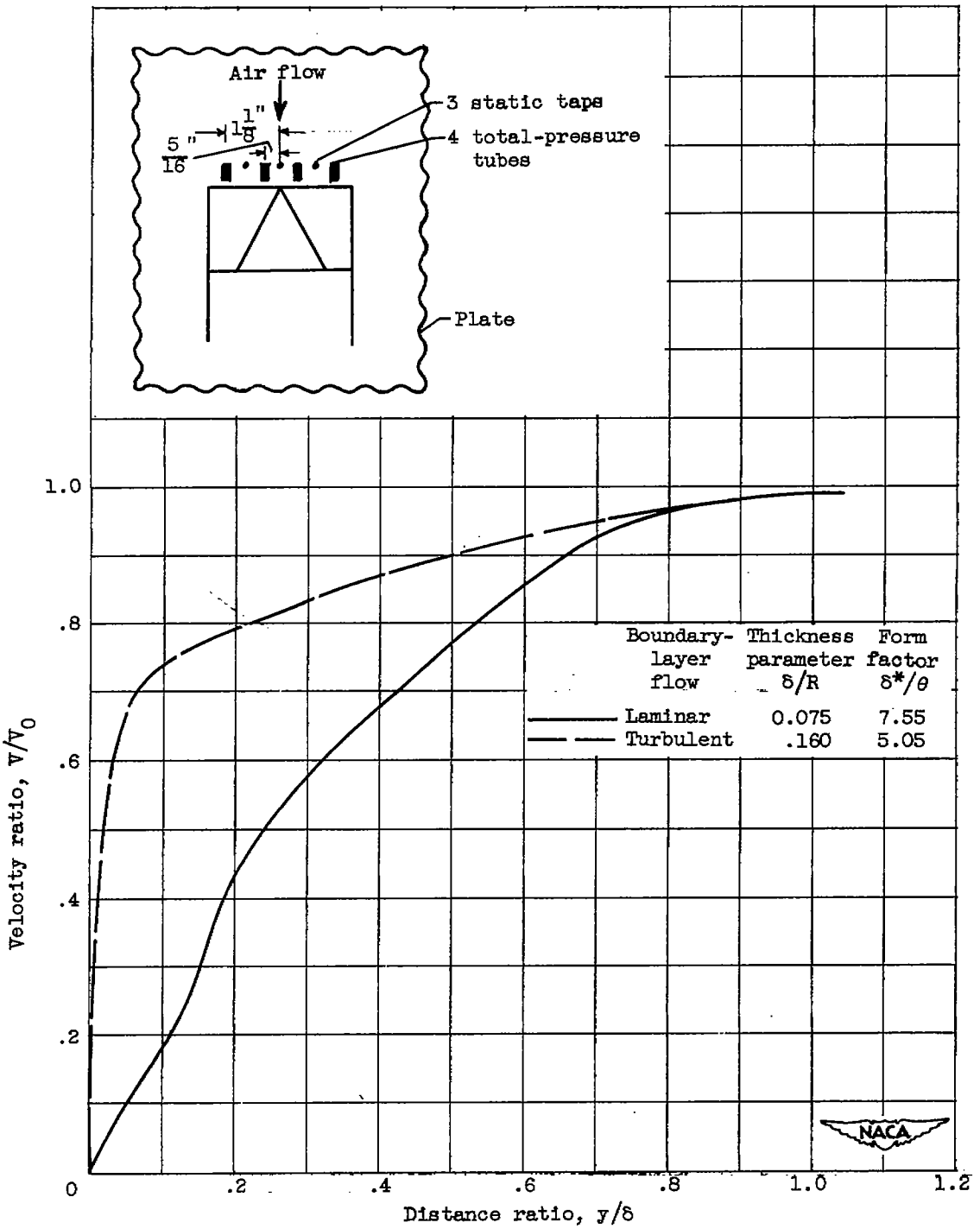

Figure 5. - Velocity profiles of two initial boundary layers.

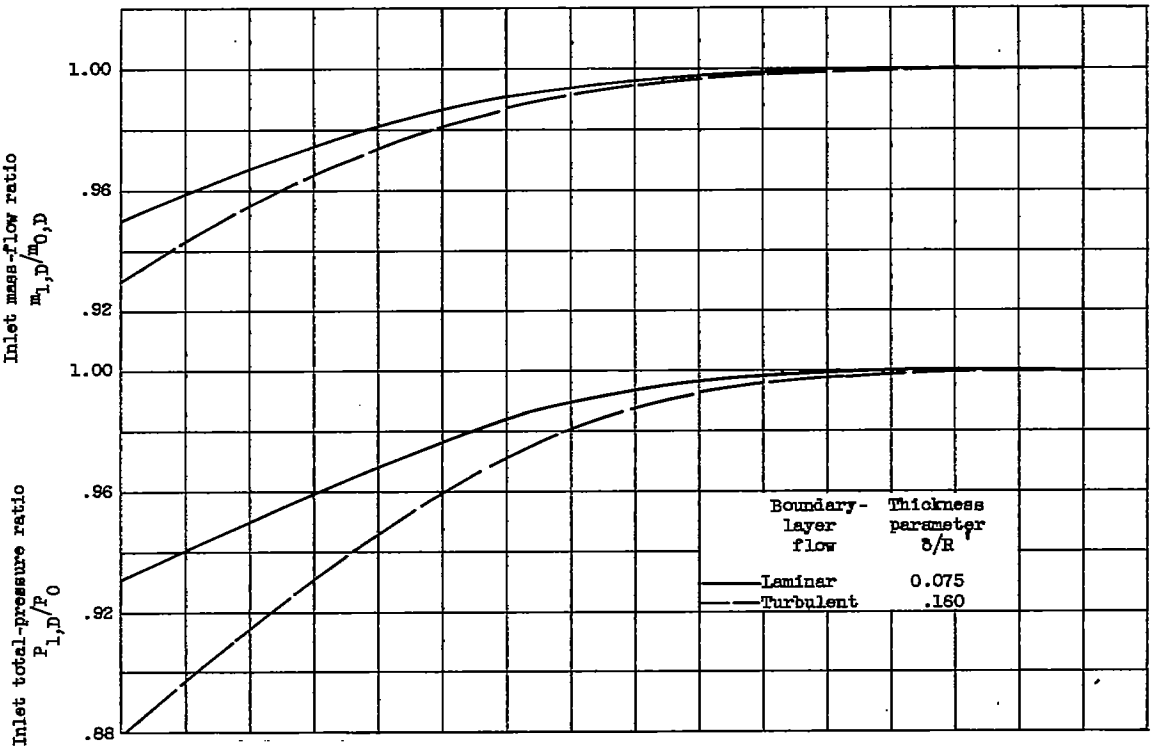

(a) Average mass-flow and total-pressure ratios upstream of inlet.

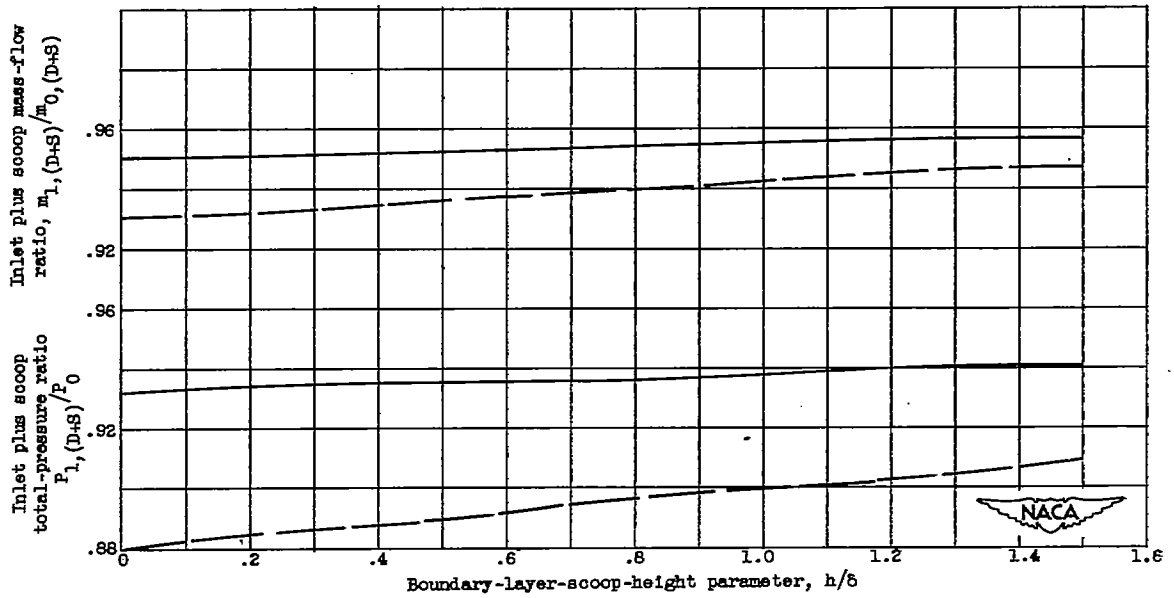

(b) Average mass-flow and total-pressure ratios upstream of combination of inlet and boundary-layer scoop.

Figure 6. - Variation of average mass-flow and total-pressure ratios at station 1.

[redacted]

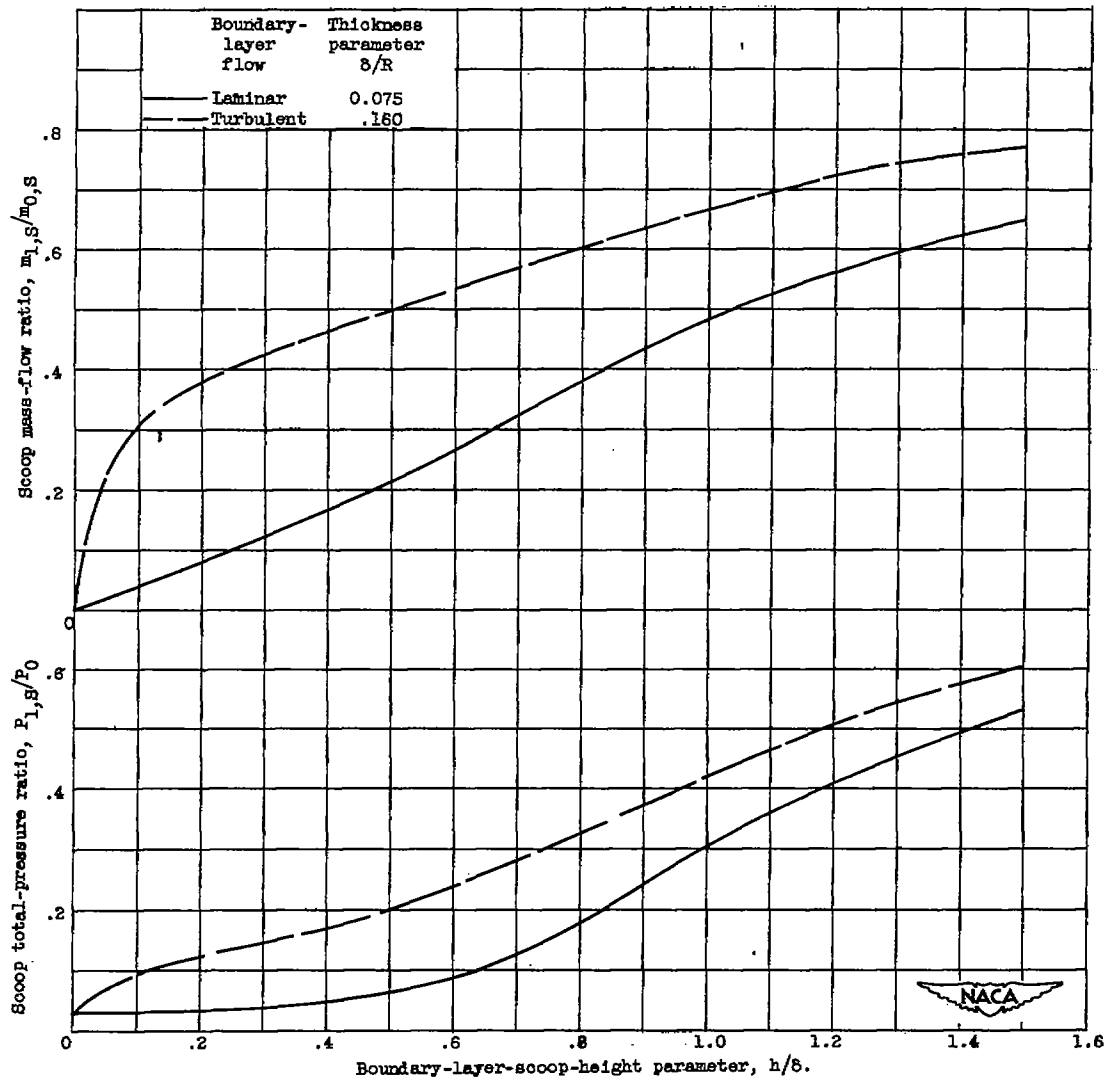

(c) Average mass-flow and total-pressure ratios upstream of boundary-layer scoop.

Figure 6. - Concluded. Variation of average mass-flow and total-pressure ratios at station 1.

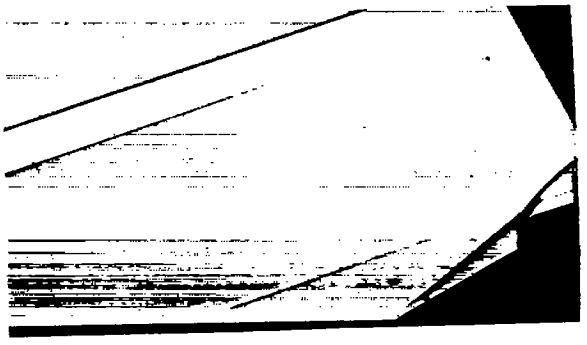

Boundary-layer-scoop-height parameter, 0; inlet total-pressure recovery, 0.367; inlet mass-flow ratio, 0.902.

Boundary-layer-scoop-height parameter, 0.509; inlet total-pressure recovery, 0.456; inlet mass-flow ratio, 0.957; scoop mass flow, supercritical.

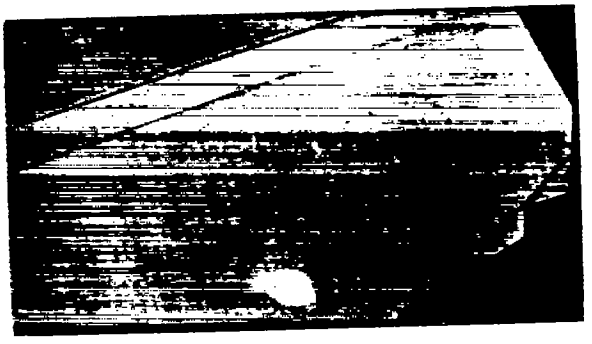

NACA C-29595

Boundary-layer-scoop-height parameter, 0.667; inlet total-pressure recovery, 0.482; inlet mass-flow ratio, 0.982; scoop mass flow, supercritical.

(a) Initial turbulent boundary layer.

Figure 7. - Steady schlieren photographs of peak-pressure configurations.

[redacted]

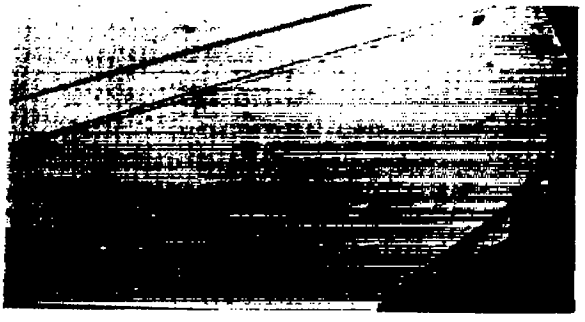

Boundary-layer-scoop-height parameter, 0.833; inlet total-pressure recovery, 0.511; inlet mass-flow ratio, 0.968; scoop mass flow, supercritical.

Boundary-layer-scoop-height parameter, 1.025; inlet total-pressure recovery, 0.488; inlet mass-flow ratio, 0.963; scoop mass flow, supercritical.

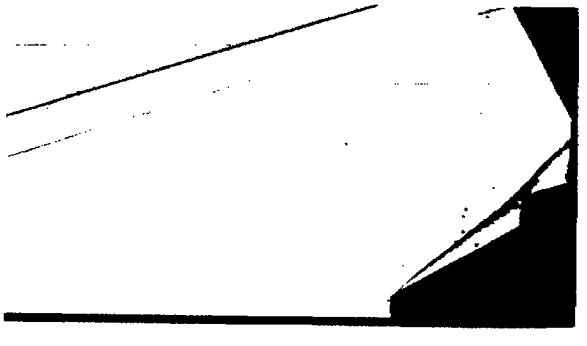

NACA C-29596

Boundary-layer-scoop-height parameter, 1.51; inlet total-pressure recovery, 0.425; inlet mass-flow ratio, 0.877; scoop mass-flow ratio, 0.655 (subcritical).

(a) Concluded. Initial turbulent boundary layer.

Figure 7. - Continued. Steady schlieren photographs of peak-pressure configurations.

[redacted]

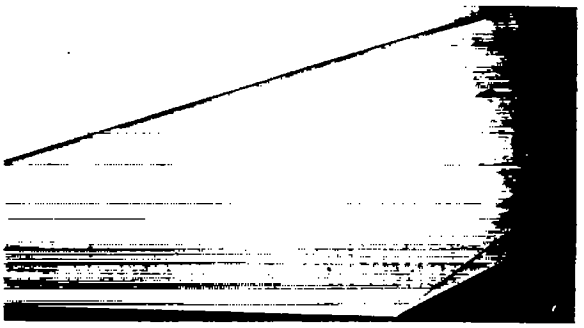

Boundary-layer-scoop-height parameter, 0; inlet total-pressure recovery, 0.397; inlet mass-flow ratio, 0.958.

Boundary-layer-scoop-height parameter, 0.362; inlet total-pressure recovery, 0.411; inlet mass-flow ratio, 0.996; scoop mass-flow ratio, 0.523 (subcritical).

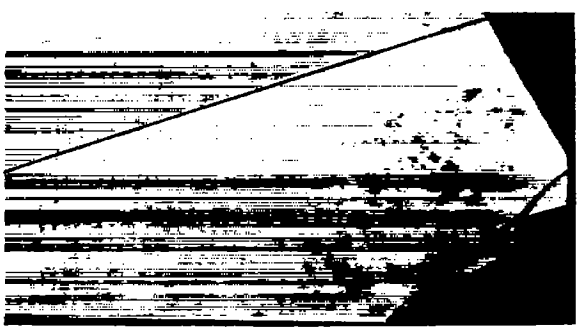

NACA C-29597

Boundary-layer-scoop-height parameter, 0.705; inlet total-pressure recovery, 0.407; inlet mass-flow ratio, 0.975; scoop mass-flow ratio, 0.181 (subcritical).

(b) Initial laminar boundary layer.

Figure 7. - Continued. Steady schlieren photographs of peak-pressure configurations.

Boundary-layer-scoop-height parameter, 1.048; inlet total-pressure recovery, 0.444; inlet mass-flow ratio, 0.965; scoop mass-flow ratio, 0.640 (subcritical).

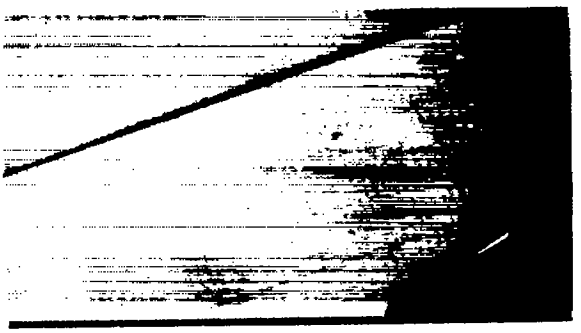

Boundary-layer-scoop-height parameter, 1.284; inlet total-pressure recovery, 0.448; inlet mass-flow ratio, 0.937; scoop mass-flow, supercritical.

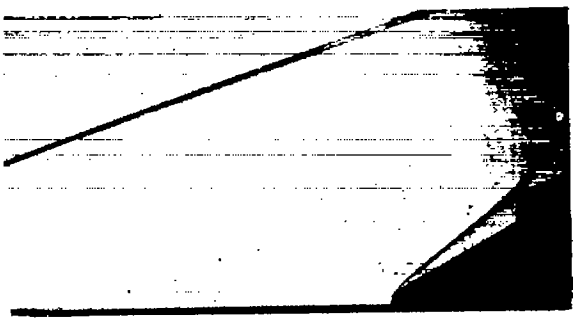

NACA
C-29598

Boundary-layer-scoop-height parameter, 1.446; inlet total-pressure recovery, 0.458; inlet mass-flow ratio, 0.950; scoop mass-flow, supercritical.

(b) Concluded. Initial laminar boundary layer.

Figure 7. - Concluded. Steady schlieren photographs of peak-pressure configurations.

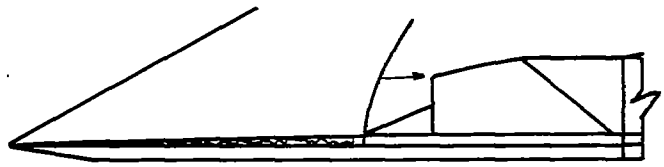

(a) Subcritical inlet flow; boundary-layer-scoop-height parameter $h/\delta > 0.833$; scoop mass-flow ratio $m_S/m_{S,max} \neq 1.0$ (supercritical).

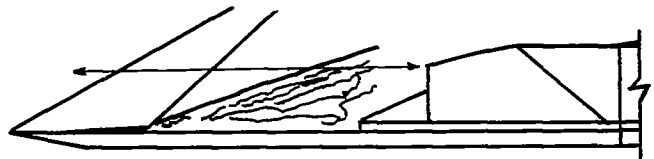

(b) Subcritical inlet flow; boundary-layer-scoop-height parameter $h/\delta > 0.833$; subcritical scoop flow.

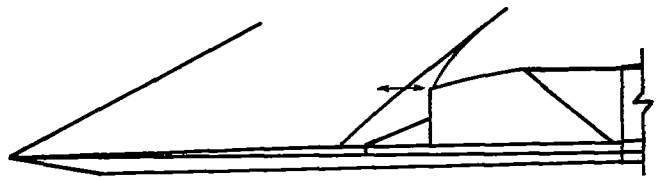

(c) Supercritical inlet flow; boundary-layer-scoop-height parameter $h/\delta > 0.833$; subcritical scoop flow.

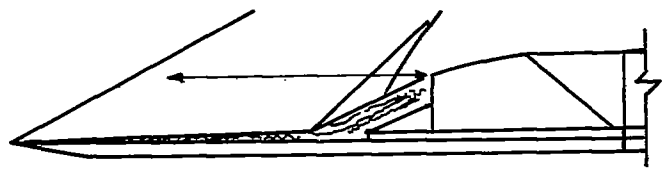

(d) Inlet oscillation induced by scoop; boundary-layer-scoop-height parameter $h/\delta > 0.833$; subcritical scoop flow.

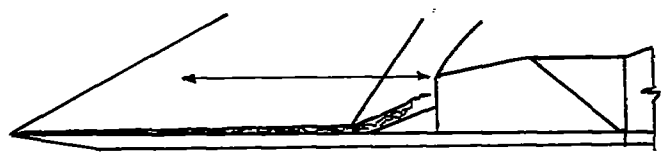

(e) Subcritical inlet flow; boundary-layer-scoop-height parameter $h/\delta = 0$.

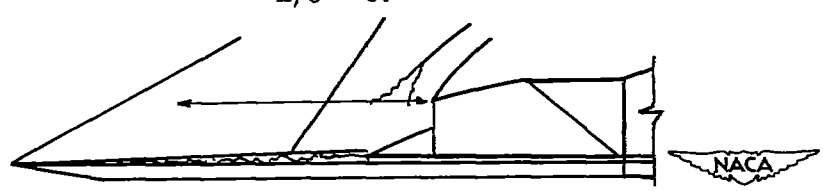

(f) Subcritical inlet flow; boundary-layer-scoop-height parameter $h/\delta = 0.509$ and 0.667; subcritical scoop flow.

Figure 8. - Buzz patterns observed for operation in turbulent boundary layer. Thickness parameter, 0.160.

[redacted]

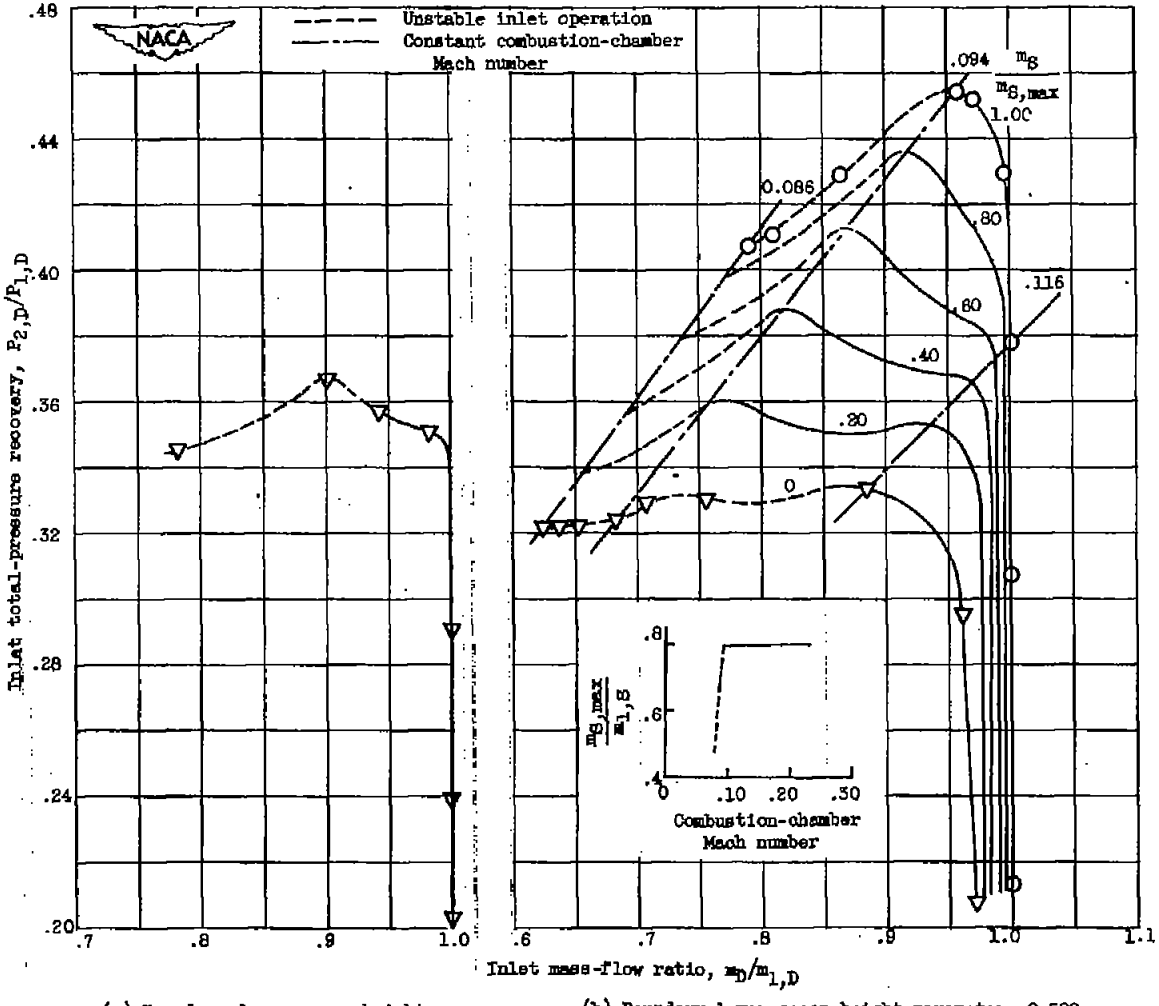

(a) Boundary-layer-scoop-height parameter, 0.

(b) Boundary-layer-scoop-height parameter, 0.509.

Figure 9. - Inlet total-pressure recovery as function of inlet mass-flow ratio for various boundary-layer-scoop heights and boundary-layer-scoop mass-flow ratios in turbulent boundary layer. Thickness parameter, 0.160.

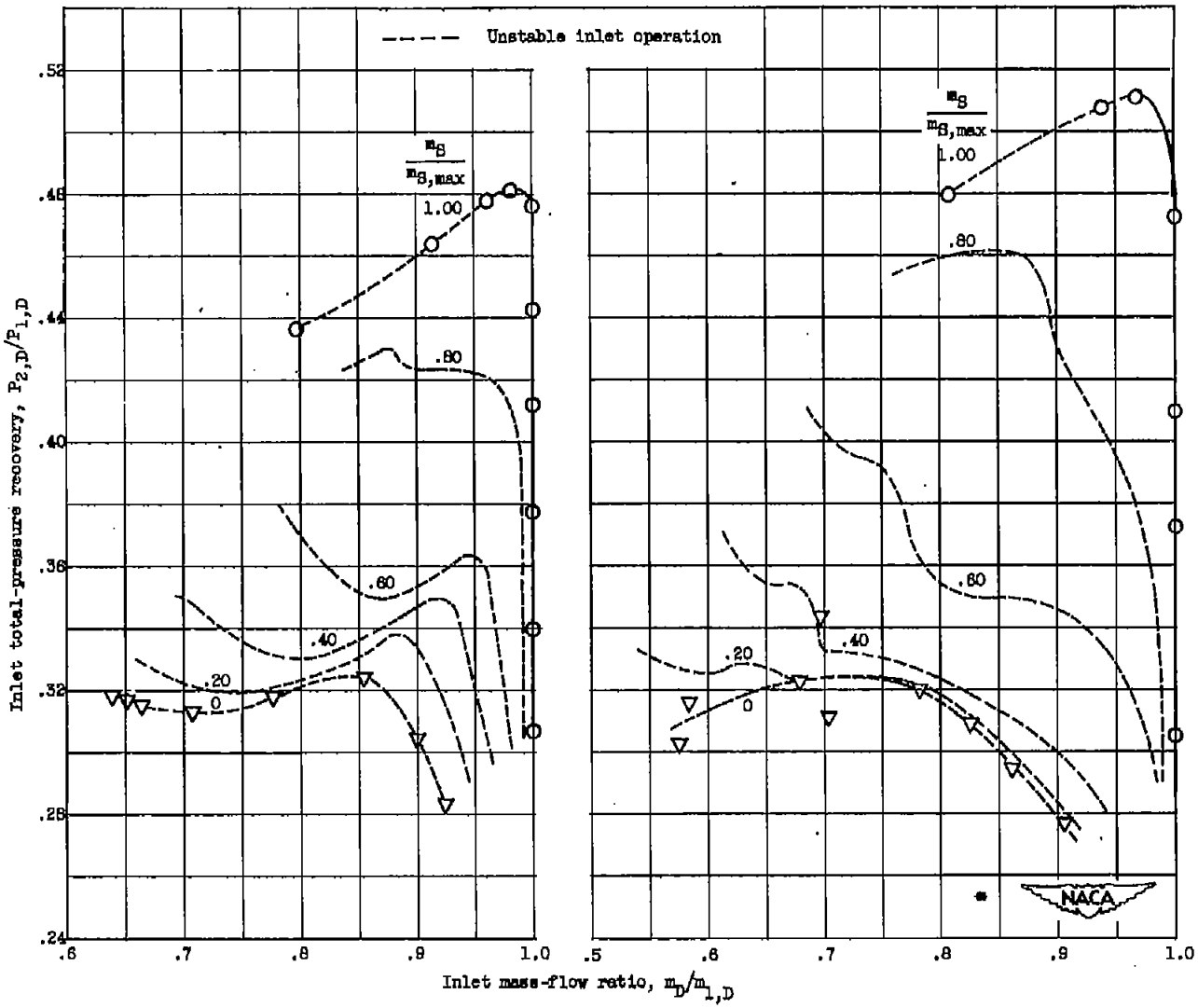

(c) Boundary-layer-scoop-height parameter, 0.667.

(d) Boundary-layer-scoop-height parameter, 0.833.

Figure 9. - Continued. Inlet total-pressure recovery as function of inlet mass-flow ratio for various boundary-layer-scoop heights and boundary-layer-scoop mass-flow ratios in turbulent boundary layer. Thickness parameter, 0.180.

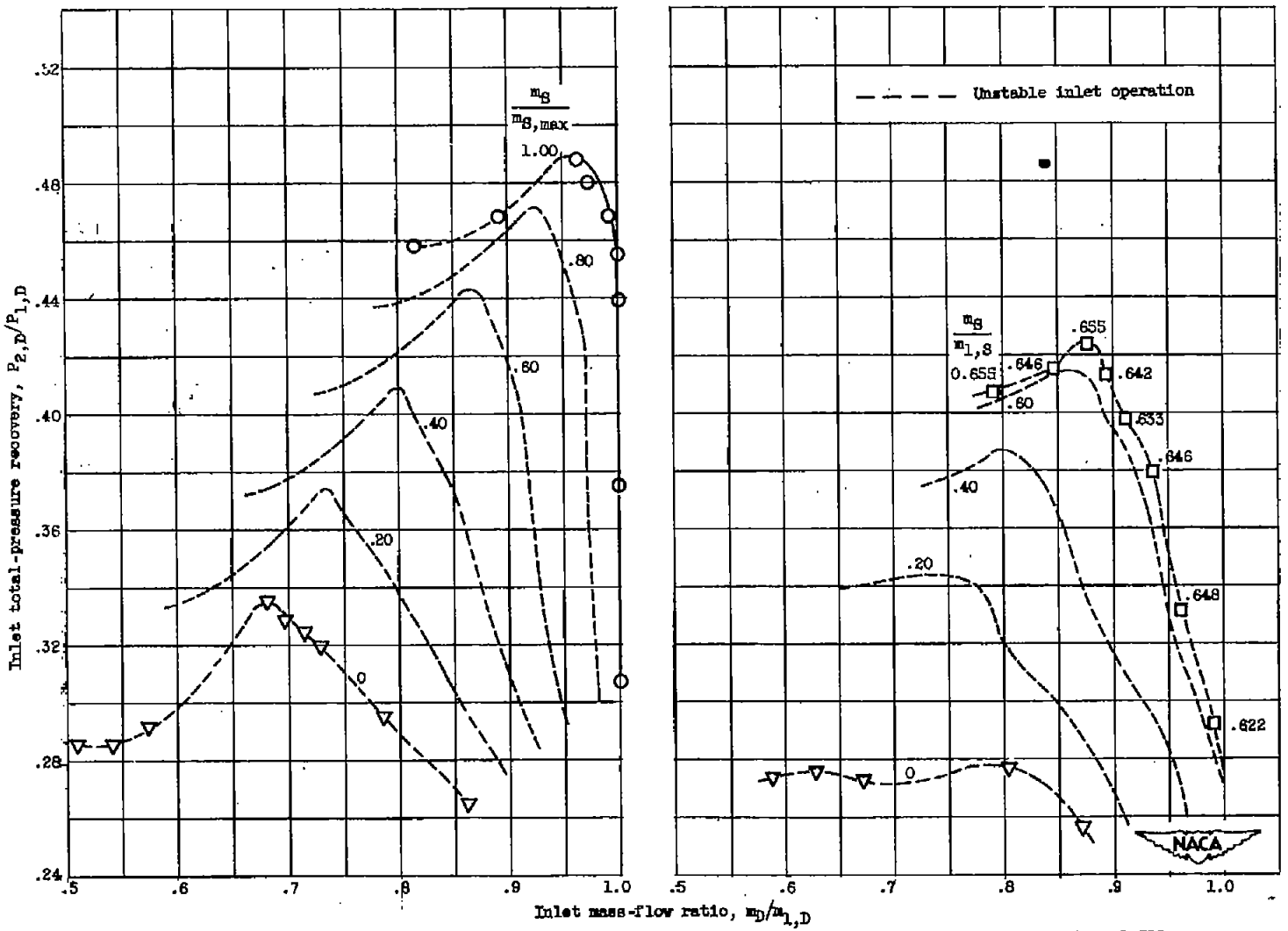

(e) Boundary-layer-scoop-height parameter, 1.025.

(f) Boundary-layer-scoop-height parameter, 1.510.

Figure 9. - Concluded. Inlet total-pressure recovery as function of inlet mass-flow ratio for various boundary-layer-scoop heights and boundary-layer-scoop mass-flow ratios in turbulent boundary layer. Thickness parameter, 0.160.

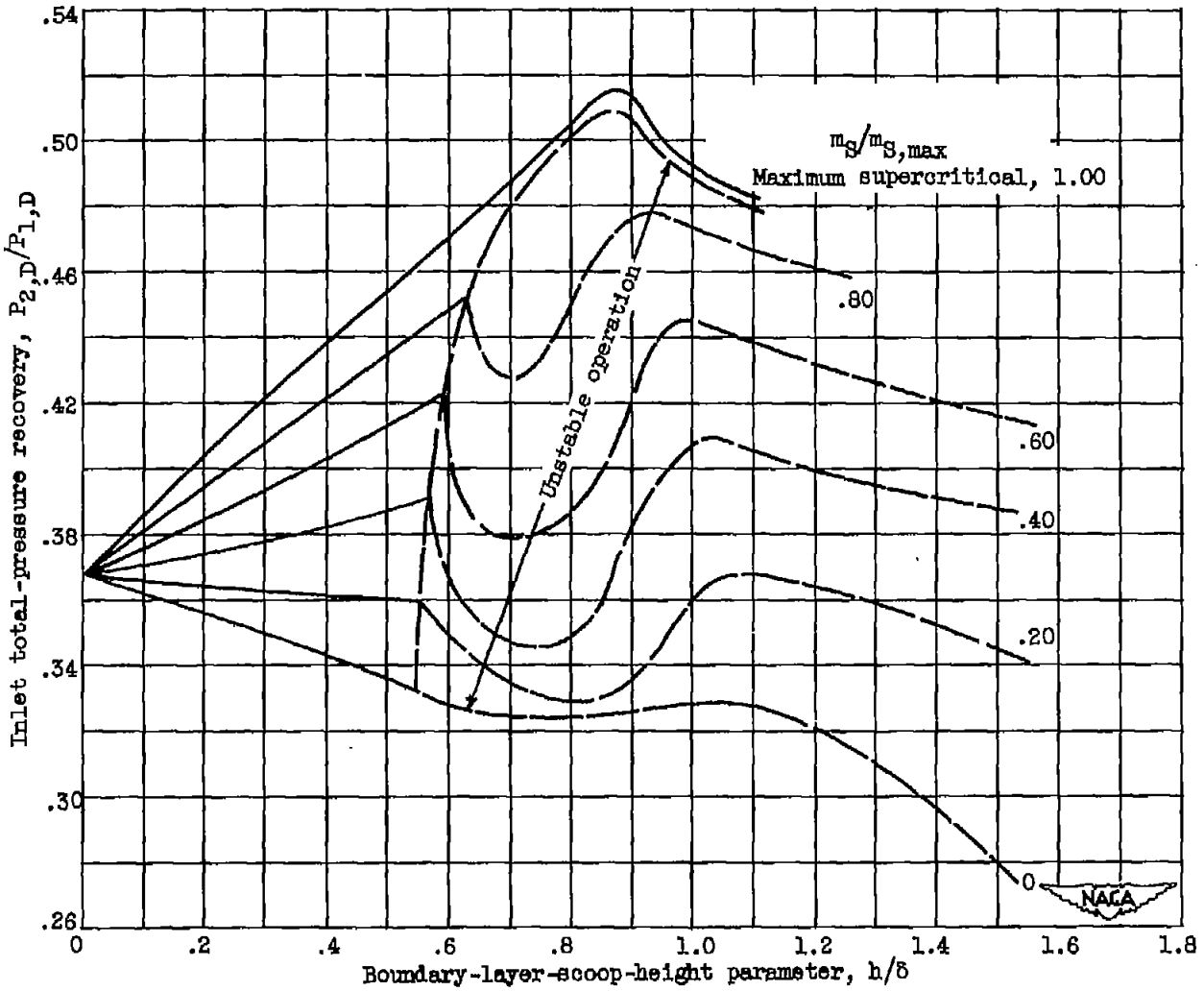

Figure 10. - Peak total-pressure recovery as function of boundary-layer-scoop-height parameter for turbulent boundary layer. Thickness parameter, 0.160.

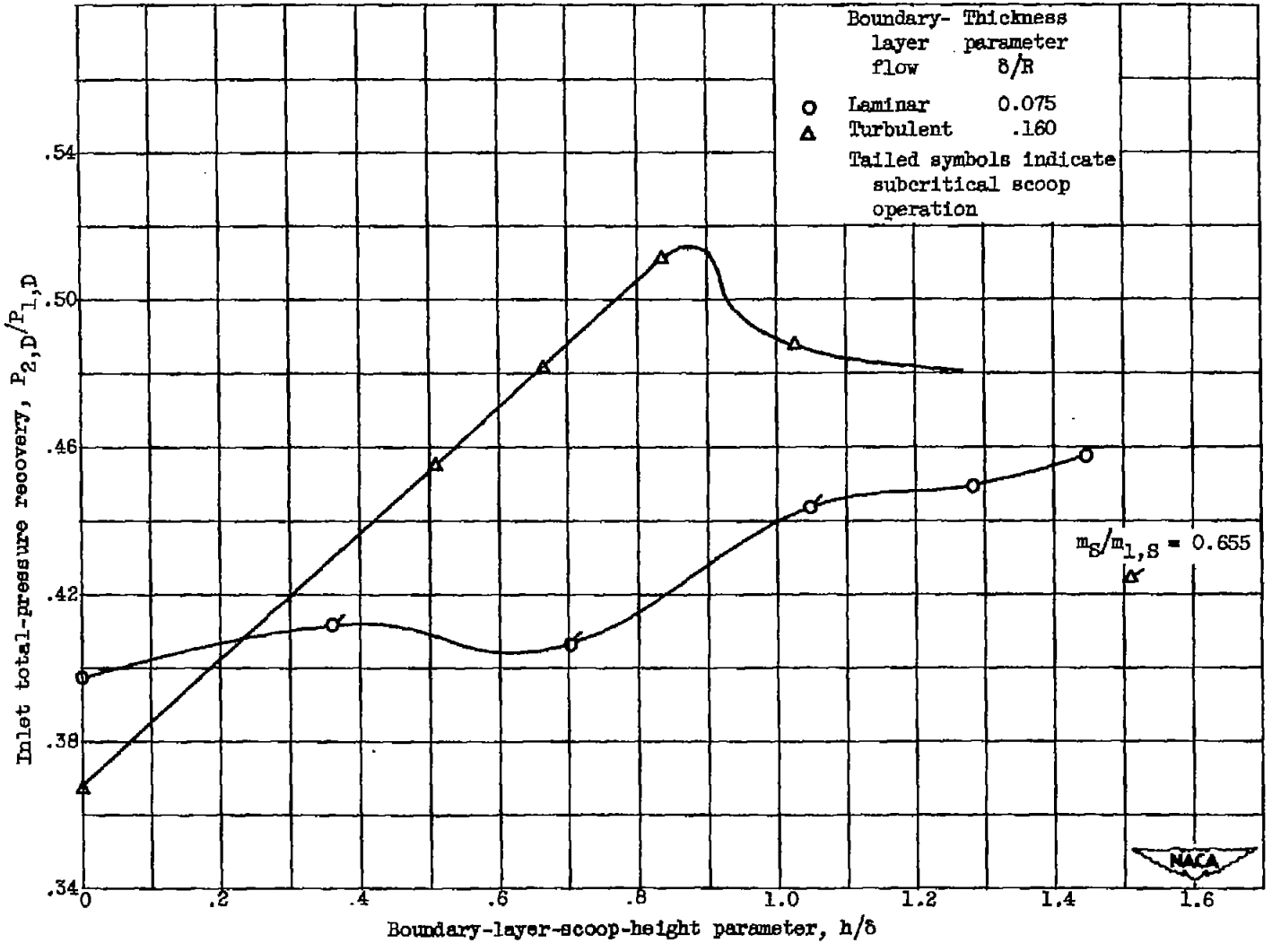

Figure 11. - Peak total-pressure recovery as function of boundary-layer-scoop-height parameter for two initial boundary layers.

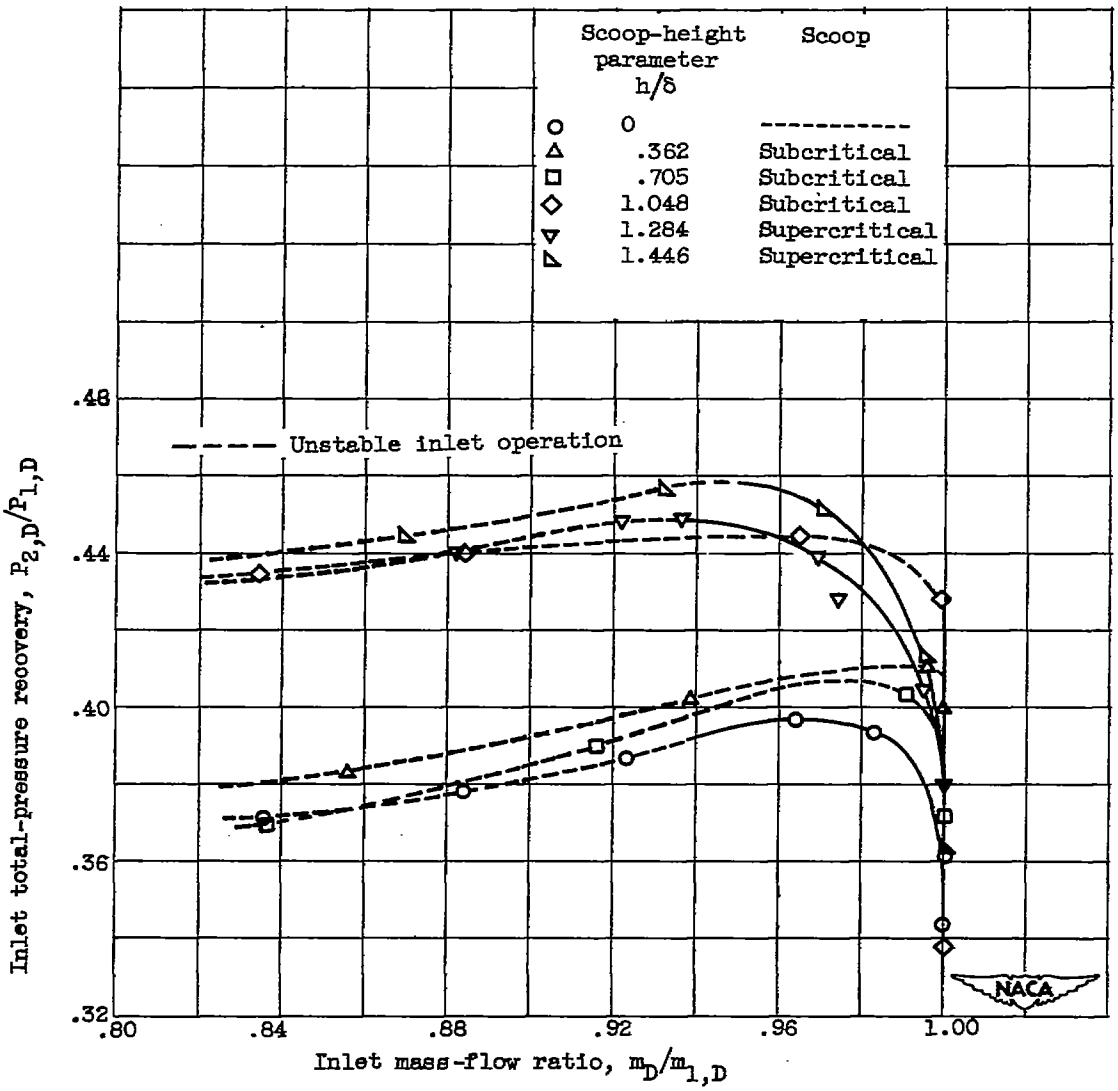

Figure 12. - Inlet total-pressure recovery as function of inlet mass-flow ratio for maximum attainable scoop mass flow. Inlet boundary-layer-thickness parameter, 0.075 (laminar).

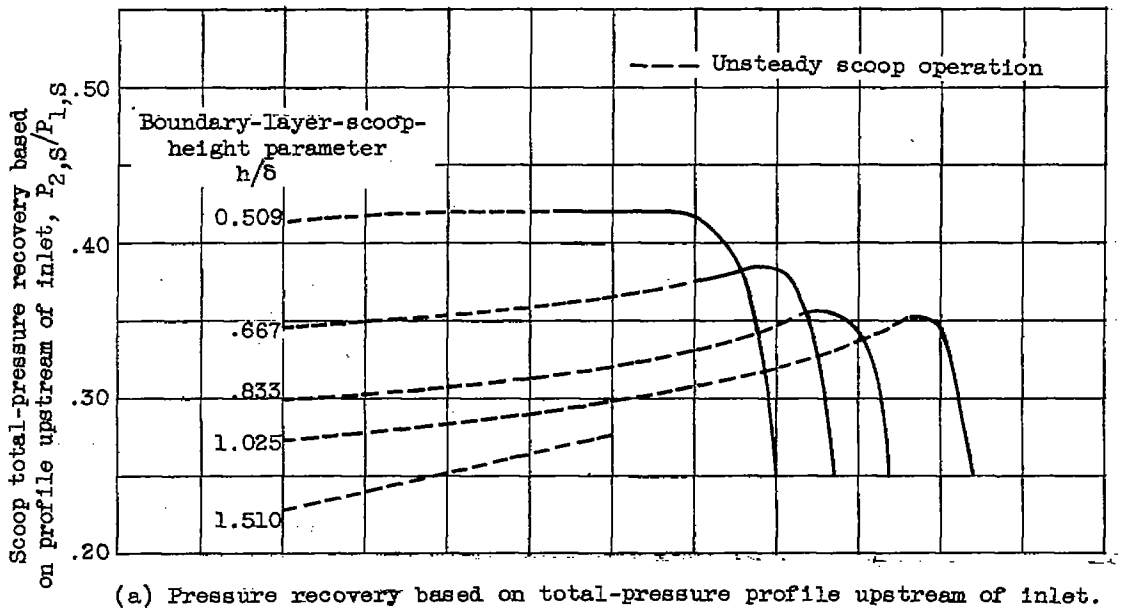

(a) Pressure recovery based on total-pressure profile upstream of inlet.

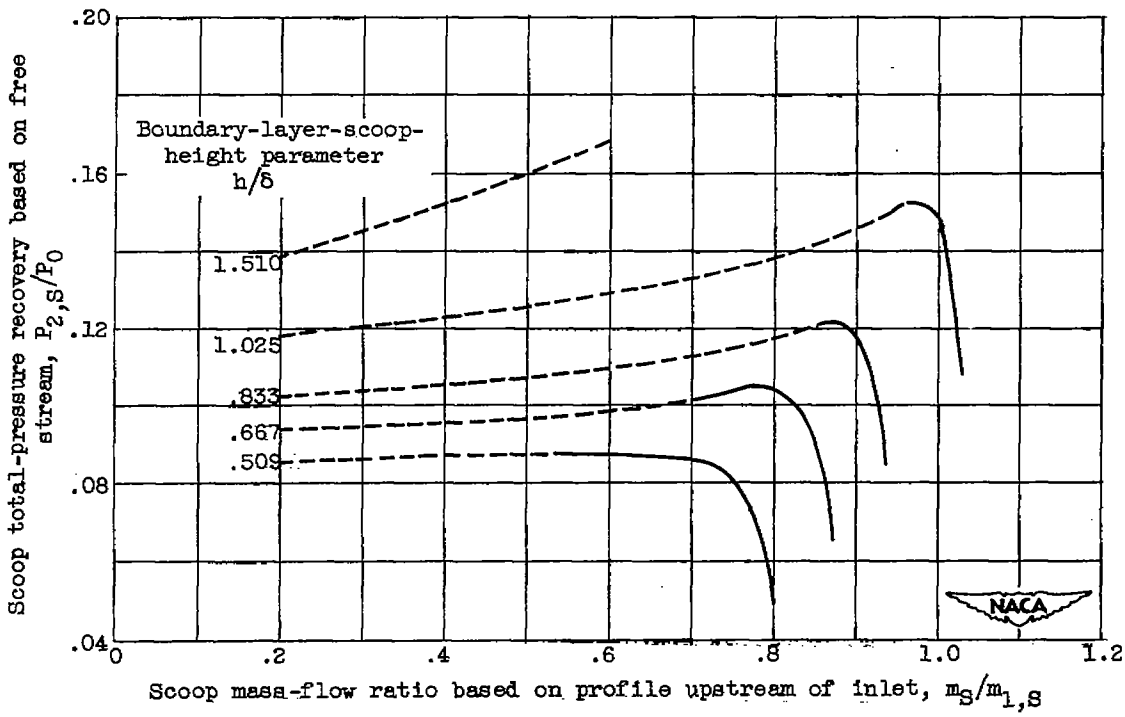

(b) Pressure recovery based on free-stream conditions.

Figure 13. - Boundary-layer-scoop pressure recovery as function of mass-flow ratio for various scoop heights. Boundary-layer-thickness parameter, 0.160 (turbulent).

[redacted]

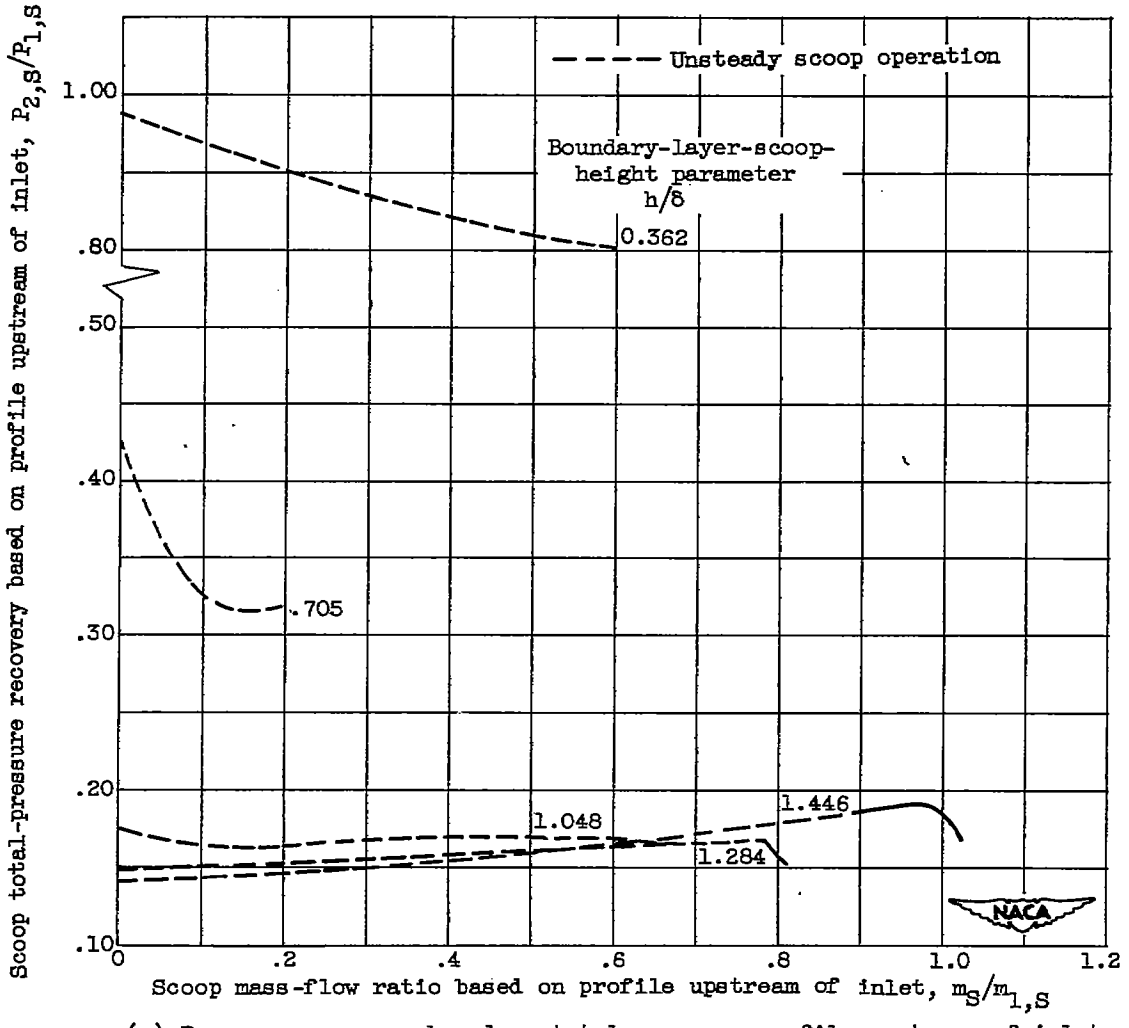

(a) Pressure recovery based on total-pressure profile upstream of inlet.

Figure 14. - Boundary-layer-scoop pressure recovery as function of mass-flow ratio for various scoop heights. Boundary-layer-thickness parameter, 0.075 (laminar).

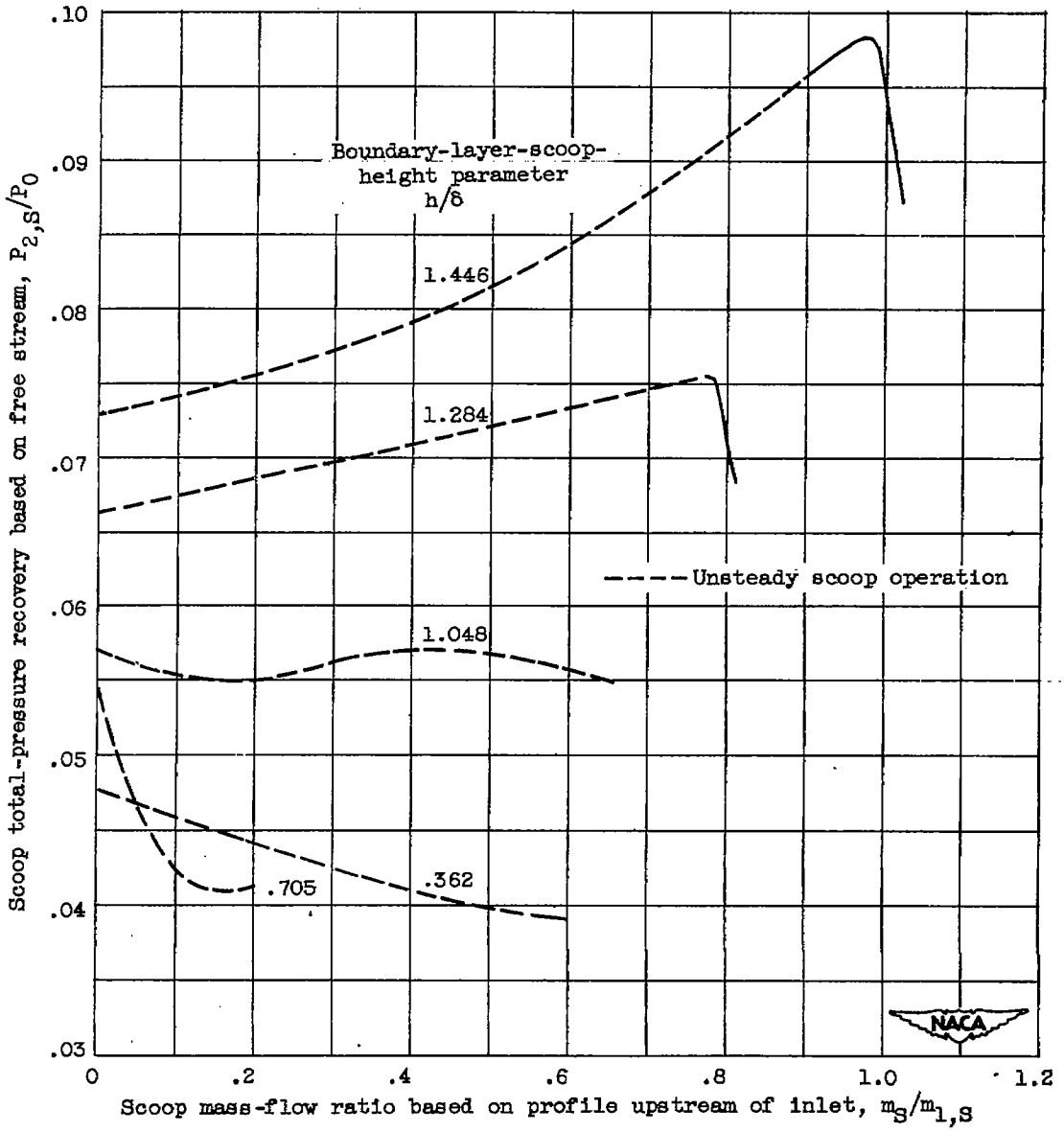

(b) Pressure recovery based on free-stream total pressure.

Figure 14. - Concluded. Boundary-layer-scoop pressure recovery as function of mass-flow ratio for various scoop heights. Boundary-layer-thickness parameter, 0.075 (laminar).

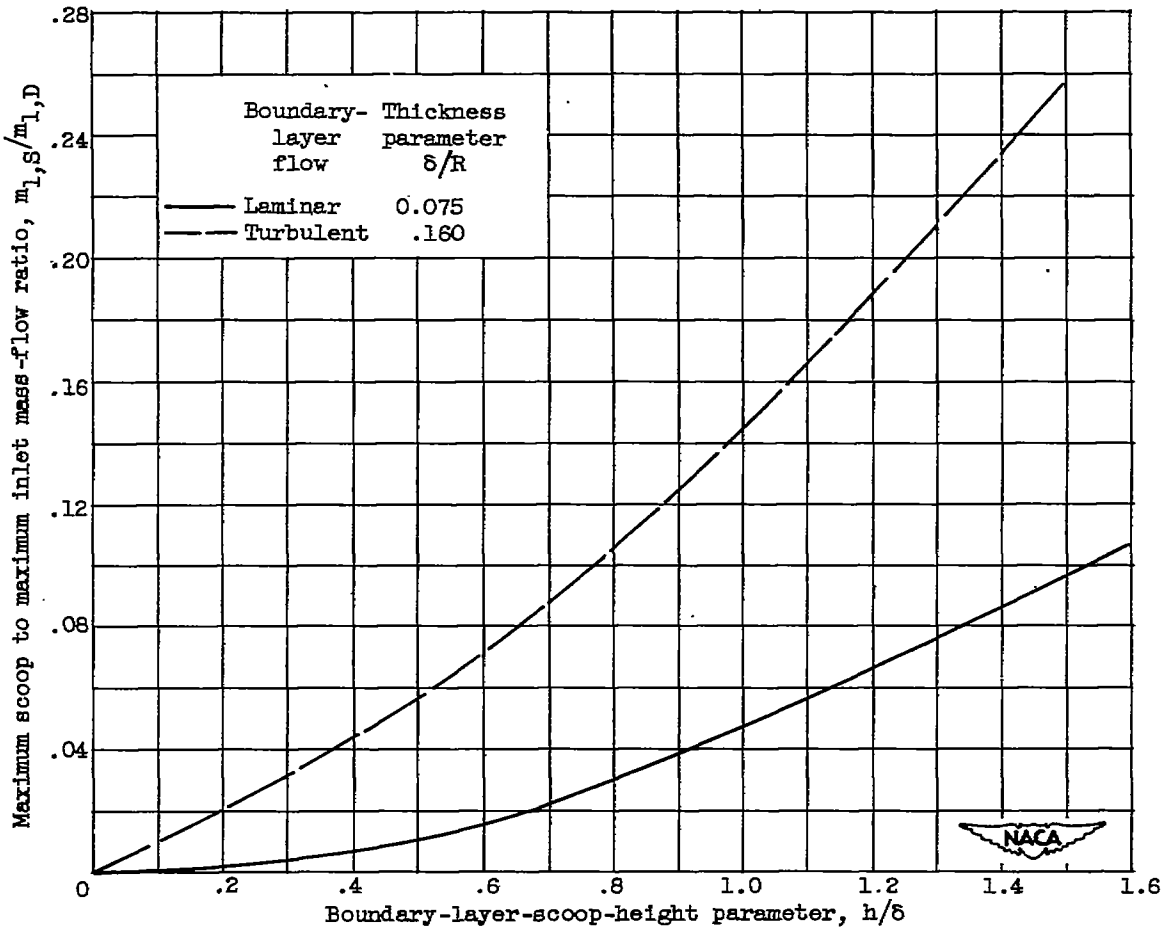

Figure 15. - Ratio of maximum scoop mass flow to maximum inlet mass flow as function of boundary-layer-scoop-height parameter for two initial boundary layers.

[redacted]

[redacted]